

Convergence Analysis of Split Learning on Non-IID Data

Yipeng Li and Xincheng Lyu *

Abstract

Split Learning (SL) is one promising variant of Federated Learning (FL), where the AI model is split and trained at the clients and the server collaboratively. By offloading the computation-intensive portions to the server, SL enables efficient model training on resource-constrained clients. Despite its booming applications, SL still lacks rigorous convergence analysis on non-IID data, which is critical for hyperparameter selection. In this paper, we first prove that SL exhibits an $\mathcal{O}(1/\sqrt{R})$ convergence rate for non-convex objectives on non-IID data, where R is the number of total training rounds. The derived convergence results can facilitate understanding the effect of some crucial factors in SL (e.g., data heterogeneity and synchronization interval). Furthermore, comparing with the convergence result of FL, we show that the guarantee of SL is worse than FL in terms of training rounds on non-IID data. The experimental results verify our theory. More findings on the comparison between FL and SL in cross-device settings are also reported.

1 Introduction

Federating Learning (FL) is a popular distributed learning paradigm where multiple clients collaborate to train a global model under the orchestration of one central server. There are two settings in FL (McMahan et al., 2017) including (i) the cross-silo setting where clients are organizations and the client number is typically less than 100 and (ii) the cross-device setting where clients are IoT devices and the client number can be up to 10^{10} (Kairouz et al., 2021). To alleviate the computation bottleneck at resource-constrained IoT devices in the cross-device scenario, Split Learning (SL) is emerged recently (Gupta and Raskar, 2018; Vepakomma et al., 2018), where the AI model is split to be trained at the clients and server separately. The computation-intensive portions are typically offloaded to the server, which is critical for the model training at resource-constrained devices. SL is regarded as one of the enabling technologies for edge intelligence in future (Zhou et al., 2019).

The comparisons of FL and SL are of practical interest for the design and deployment of intelligent networks. Existing studies focus on various aspects for their comparisons (Thapa et al., 2020; Gao et al., 2020, 2021), e.g., in terms of learning performance (Gupta and Raskar, 2018), computation efficiency (Vepakomma et al., 2018), communication overhead (Singh et al., 2019), and privacy issues (Thapa et al., 2021). For example, with the emphasis on the learning performance comparison, Gao et al. (2020, 2021) find that SL exhibits (i) faster convergence speed than FL under IID data in terms of communication rounds; (ii) better learning performance under imbalanced data; (iii) worse

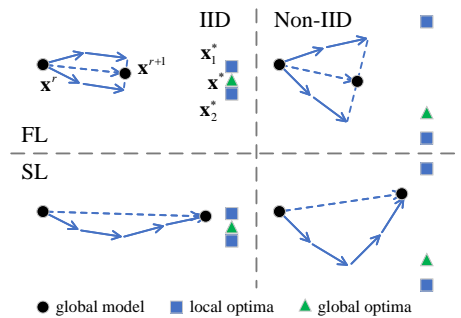


Figure 1: Illustration of the model updates of FL and SL for 2 clients and 2 local update steps in one round.

*Email: {liyipeng, lvxincheng}@bupt.edu.cn. Beijing University of Posts and Telecommunications, China.

learning performance under (extreme) non-IID data, etc.

The difference arises from the distinct process of model updates of FL and SL. In particular, FL takes the average of the local model parameters at the end of each round; SL trains the clients in sequence and does not average the client updates. Figure 1 plots the client drift (Karimireddy et al., 2020; Wang et al., 2020; Li et al., 2022) of FL and SL under both IID and non-IID data to visualize the update process. Under the IID setting, SL approaches the global optima \mathbf{x}^* faster than FL given the sequential training mechanism. In contrast, under the non-IID setting, SL may deviate from the global optima for the same reason.

Convergence analysis is critical for the performance comparison between SL and FL. Specifically, a rigorous analysis is of importance for the vital research questions raised by (Gao et al., 2020) (which are only empirically evaluated but remain unsolved in theory): RQ1-“*What factors affect SL performance?*” and RQ2-“*In which setting will the SL performance outperform FL?*”. A wealth of work has analyzed the convergence of FL in the cases of IID (Stich, 2019; Zhou and Cong, 2017; Khaled et al., 2020), non-IID (Li et al., 2020, 2019; Khaled et al., 2020; Karimireddy et al., 2020) and unbalanced data (Wang et al., 2020). However, with the distinct update process, the convergence analysis of SL has yet to be solved on non-IID data. To this end, this paper first derives a rigorous convergence results of SL and draw the comparison results of FL and SL theoretically.

The main contributions can be summarized with respect to the two research questions above:

- We prove the convergence of SL on non-IID data with the standard assumptions used in the FL literature¹ with a convergence rate of $\mathcal{O}(1/\sqrt{R})$ in Section 4.2. By this, we find that the convergence of SL is affected by factors such as data heterogeneity and synchronization interval. Experimental results verify the analysis results empirically in Section 5.2. To the best of our knowledge, this work is the first to give the convergence analysis of SL on non-IID data.
- We compare FL² and SL in theory (Section 4.3) and in practice (Section 5.3). The theory shows that (i) the best and threshold learning rate of SL is smaller than FL (ii) and the guarantee of SL is worse than FL in terms of training rounds on non-IID data, which have been verified empirically. However, our experiments also show that SL can outperform FL when the synchronization interval is small on non-IID data in the cross-device settings.

2 Preliminaries

As two of the most popular distributed learning frameworks, both FL and SL aim to train the global model from distributed datasets. The optimization problem of FL and SL with N clients can be given by

$$\min_{\mathbf{x} \in \mathbb{R}^d} \left\{ f(\mathbf{x}) := \sum_{i=1}^N p_i f_i(\mathbf{x}) \right\}, \quad (1)$$

where $p_i = n_i/n$ is the ratio of local samples at client i (n and n_i are the sizes of the overall dataset \mathcal{D} and local dataset \mathcal{D}_i at client i , respectively), \mathbf{x} is the model parameters, $f(\mathbf{x})$ is the global objective, $f_i(\mathbf{x})$ denotes the local objective function at client i . In particular, $f_i(\mathbf{x}) := \mathbb{E}_{\delta_i \sim \mathcal{D}_i} [f_i(\mathbf{x}; \delta_i)] = \frac{1}{n_i} \sum_{\delta_i \in \mathcal{D}_i} \ell(\mathbf{x}; \delta_i)$, where $\ell(\mathbf{x}; \delta_i)$ is the loss computed on the model parameter \mathbf{x} and data sample δ_i from \mathcal{D}_i .

¹We only show the convergence for non-convex objective functions here since SL is now often used in large deep learning models whose objective functions are possibly non-convex. Nevertheless, similar methods can be used to get the convergence for general convex functions and strongly convex functions.

²We use FedAvg (McMahan et al., 2017) as the baseline algorithm of FL for comparison in this work.

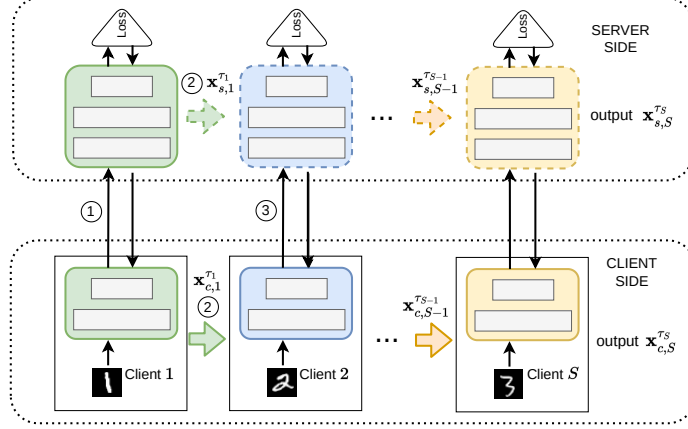


Figure 2: Overview of vanilla SL (the peer-to-peer mode (Gupta and Raskar, 2018)). The first three steps of the workflow: ① the local training on the local dataset of client 1 (steps 5-11 of Algorithm 1); ② the client-side model synchronization of clients 1 and 2, i.e., client 1 sends the client-side local model parameters to client 2; ③ the local training on the local dataset of client 2. Note that there is only one server-side model in the sever side. Here we use the dashed arrows and rectangles to show the updates of the server-side model to make the process of SL clear.

Setup of SL. Figure 2 demonstrates the relay-based (sequential) training process of the vanilla SL. The details are shown in Algorithm 1. Considering the massive number of clients in cross-device setting, only a subset \mathcal{S} of clients are selected for model training at each round (step 2 of Algorithm 1). The update order of the selected clients can be meticulously designed or randomly determined (used in this paper). The i -th client requests and initializes with the lasted model (step 4). Then the client and server cooperate to perform multiple local updates (steps 5-11). Since the client updates the client-side local model and the sever updates the server-side local model synchronously, without loss of generality, the local update processes of both can be written as one formula (steps 4, 10):

$$\begin{cases} \text{Initialize:} & \mathbf{x}_i^{(r,0)} = \begin{cases} \mathbf{x}^r, i = 1 \\ \mathbf{x}_{i-1}^{(r,\tau_{i-1})}, i > 1 \end{cases} \\ \text{Update:} & \mathbf{x}_i^{(r,k+1)} = \mathbf{x}_i^{(r,k)} - \eta \mathbf{g}_i(\mathbf{x}_i^{(r,k)}), \end{cases} \quad (2)$$

where \mathbf{x}^r is the full global model (parameters) in the r -th round, $\mathbf{x}_i^{(r,k)}$ denotes the full local model after the k -th local update on the local dataset \mathcal{D}_i in the r -th round, η is the learning rate and $\mathbf{g}_i(\mathbf{x}_i^{(r,k)}) := \nabla f_i(\mathbf{x}_i^{(r,k)}; \xi_i^{(r,k)})$ denotes the stochastic gradients of f_i computed on the model parameter $\mathbf{x}_i^{(r,k)}$ and mini-batch $\xi_i^{(r,k)}$ sampled randomly from \mathcal{D}_i . Note that the full local model $\mathbf{x}_i^{(r,k)}$ consists of the client-side local model $\mathbf{x}_{c,i}^{(r,k)}$ and server-side local model $\mathbf{x}_{s,i}^{(r,k)}$.

After τ_i local updates, the client i will send the model parameters to the next client (i.e., the $i+1$ -th client), where τ_i is the synchronization interval or number of local update steps of client i . This process is called the client-side model synchronization. After the server and the last client in \mathcal{S} (i.e., the S -th client, $S = |\mathcal{S}|$) complete their local updates, Algorithm 1 outputs the full local model $\mathbf{x}_S^{(r,\tau_S)}$ as the full global model \mathbf{x}^{r+1} for next round.

The communication of Algorithm 1 concentrates on the steps 4, 6 and 8. For brevity, we have omitted some unconcerned details of SL, e.g., the security and privacy settings.

Setup of FL. Unlike SL, clients in FL own the full AI model. In each round, a subset \mathcal{S} of clients are selected for training. After receiving the global model from the server, selected clients perform local updates in parallel. The local update process of any client i can be written as:

$$\begin{cases} \text{Initialize:} & \mathbf{x}_i^{(r,0)} = \mathbf{x}^r \\ \text{Update:} & \mathbf{x}_i^{(r,k+1)} = \mathbf{x}_i^{(r,k)} - \eta \mathbf{g}_i(\mathbf{x}_i^{(r,k)}), \end{cases} \quad (3)$$

where \mathbf{x}^r , $\mathbf{x}_i^{(r,k)}$, η , $\mathbf{g}_i(\mathbf{x}_i^{(r,k)})$ have the same meaning as SL. Then the client i sends the updated model parameters $\mathbf{x}_i^{(r,\tau_i)}$ to the server. The server aggregates the received local model parameters to generate the global model for next round as $\mathbf{x}^{r+1} = \sum_{i \in \mathcal{S}} \frac{p_i}{\sum_{i \in \mathcal{S}} p_i} \mathbf{x}_i^{(r,\tau_i)}$.

Algorithm 1 Vanilla Split Learning

Some notations:

- \mathbf{x}_c , \mathbf{x}_s denote the client-side, server-side model (parameters) respectively
- $\mathbf{x} := [\mathbf{x}_c; \mathbf{x}_s]$ denotes the full model (parameters)
- \mathbf{A} is the activation vectors of the cut layer
- $\mathbf{g}(\mathbf{A}; \mathbf{x})$ is the stochastic gradients of \mathbf{A} conditioning on the model \mathbf{x}

```

1: for training round  $r = 0, \dots, R - 1$  do
2:   Sample a subset  $\mathcal{S}$  of clients and determine their update order
3:   for client index  $i = 1, \dots, |\mathcal{S}|$  in sequence do
4:     Client  $i$ : Initialize with the latest client-side model  $\mathbf{x}_{c,i}^{(r,0)} \leftarrow \begin{cases} \mathbf{x}_c^r, i = 1 \\ \mathbf{x}_{c,i-1}^{(r,\tau_{i-1})}, i > 1 \end{cases}$ 
5:     for local update step  $k = 0, \dots, \tau_i - 1$  do
6:       Client  $i$ : Forward propagation and send  $\mathbf{A}_i^{(r,k)}$  to the server
7:       Server: Forward propagation with activations from the client
8:       Server: Back-propagation and send  $\mathbf{g}_i(\mathbf{A}_i^{(r,k)}; \mathbf{x}_i^{(r,k)})$  to the client
9:       Client  $i$ : Back-propagation with gradients from the server
10:      Local model updates:  $\begin{cases} \textbf{Client } i: & \mathbf{x}_{c,i}^{(r,k+1)} \leftarrow \mathbf{x}_{c,i}^{(r,k)} - \eta \mathbf{g}_i(\mathbf{x}_{c,i}^{(r,k)}) \\ \textbf{Server:} & \mathbf{x}_{s,i}^{(r,k+1)} \leftarrow \mathbf{x}_{s,i}^{(r,k)} - \eta \mathbf{g}_i(\mathbf{x}_{s,i}^{(r,k)}) \end{cases}$ 
11:    end for
12:  end for
13: end for
```

3 Related work

Variants of SL. SL is deemed as one promising paradigm for distributed model training at resource-constrained devices, given its computational efficiency on the client side. Most existing works focus on reducing the training delay arising from the relay-based training manner of vanilla SL in the multi-user scenario. **SplitFed** (Thapa et al., 2020) is one popular model parallel algorithm that combines the strengths of FL and SL, where each client has one corresponding instance of server-side model in the *main server* to form a pair. Each pair constitutes a full model and conducts the local updates in parallel. After each training round, the *fed server* collects and aggregates on the client-side local updates. The aggregated client-side model will be disseminated to all the clients before next round. The *main server* does the same operations to the instances of the server-side model. **SplitFedv2** (Thapa et al., 2020), **SplitFedv3** (Gawali et al., 2020) and **SFLG** (Gao et al.,

2021), FedSeq (Zaccone et al., 2022) are the variants of SplitFed. In particular, SFLG (Gao et al., 2021) is one generalized variants of SplitFed, combining SplitFed and SplitFedv2.

Convergence analysis of SL. In the case of IID data, the convergence analysis of SL is identical to standard Minibatch-SGD (Wang et al., 2022; Park et al., 2021), so some convergence properties of Minibatch SGD is applied to SL too. The algorithm in Han et al. (2021) reduces the latency and downlink communication on SplitFed by adding auxiliary networks at client-side for quick model updates. Their convergence analysis combines the theories of Belilovsky et al. (2020) and FedAvg. Wang et al. (2022) proposed FedLite to reduce the uplink communication overhead by compressing activations with product quantization and provided the convergence analysis of FedLite. However, their convergence recovers that of Minibatch SGD when there is no quantization. SGD with biased gradients (Ajalloeian and Stich, 2020) is also related. However, it only converges to a neighborhood of the solution. Furthermore, we find that Woodworth et al. (2020a,b) compared the convergence of distributed Minibatch SGD and local SGD under homogeneous and heterogeneous settings, respectively. To differentiate our work, we show how these algorithms operate in Appendix A. As a result, the convergence of SL on non-IID data is still lacking.

4 Convergence Analysis of SL

4.1 Assumptions

We make the following standard assumptions on the local objective functions $\{f_i(\mathbf{x})\}_{i=1}^N$.

Assumption 1 (*L-Smoothness*). *Each local objective function f_i is L -smooth, $i \in \{1, 2, \dots, N\}$, i.e., there exists a constant $L > 0$ such that $\|\nabla f_i(\mathbf{x}) - \nabla f_i(\mathbf{y})\| \leq L \|\mathbf{x} - \mathbf{y}\|$ for all \mathbf{x} and \mathbf{y} .*

Assumption 2 (*Unbiased gradient and bounded variance*). *For each client i , $i \in \{1, 2, \dots, N\}$, the stochastic gradient $\mathbf{g}_i(\mathbf{x}) := \nabla f_i(\mathbf{x}; \xi_i)$ is unbiased $\mathbb{E}[\mathbf{g}_i(\mathbf{x})] = \nabla f_i(\mathbf{x})$ and has bounded variance $\mathbb{E}_{\xi_i}[\|\mathbf{g}_i(\mathbf{x}) - \nabla f_i(\mathbf{x})\|^2] \leq \sigma^2$.*

Assumption 3 (*Bounded dissimilarity*). *There exist constants $B \geq 1$ and $G \geq 0$ such that $\frac{1}{N} \sum_{i=1}^N \|\nabla f_i(\mathbf{x})\|^2 \leq B^2 \|\nabla f(\mathbf{x})\|^2 + G^2$. In the IID case, $B = 1$ and $G = 0$, since all the local objective functions are identical to each other. In the non-IID case, B and G measure the heterogeneity of data distribution.*

4.2 Convergence Result and Discussion

Without loss of generality, the unweighted global objective function $f(\mathbf{x}) = \frac{1}{N} \sum_{i=1}^N f_i(\mathbf{x})$ is adopted. Moreover, we assume that each client participates in the training per round ($|\mathcal{S}| = N$) and has the same synchronization interval ($\tau_i = \tau_j = K, \forall i \neq j$ and $i, j \in [N]$) for FL and SL. Then following the proof of Wang et al. (2020); Karimireddy et al. (2020); Khaled et al. (2020), we give the convergence results of SL (details are in Appendix C), as follows:

Theorem 1. *Let Assumptions 1, 2 and 3 hold. Suppose that the learning rate satisfies $\eta \leq \frac{1}{2NKL\sqrt{2B^2+1}}$. For Algorithm 1, it holds that*

$$\mathbb{E}[\|\nabla f(\bar{\mathbf{x}}^R)\|^2] \leq \underbrace{\frac{4[f(\mathbf{x}^0) - f(\mathbf{x}^*)]}{\eta N K R}}_{T_1: \text{initialization error}} + \underbrace{12\eta^2 N^2 K^2 L^2 G^2 + 6\eta^2 N^2 K L^2 \sigma^2}_{T_2: \text{client drift error}} + \underbrace{4\eta N L \sigma^2}_{T_3: \text{global variance}}, \quad (4)$$

where $\bar{\mathbf{x}}^R = \frac{1}{R} \sum_{r=0}^{R-1} \mathbf{x}^r$ is the averaged global model over the R rounds.

Corollary 1. Choose $\eta = \frac{1}{NK\sqrt{R}}$ and apply the result of Theorem 1. For sufficiently large R , it holds that

$$\mathbb{E}[\|\nabla f(\bar{\mathbf{x}}^R)\|^2] \leq \underbrace{\mathcal{O}\left(\frac{F}{\sqrt{R}}\right)}_{T_1: \text{initialization error}} + \underbrace{\mathcal{O}\left(\frac{KG^2 + \sigma^2}{KR}\right)}_{T_2: \text{client drift error}} + \underbrace{\mathcal{O}\left(\frac{\sigma^2}{K\sqrt{R}}\right)}_{T_3: \text{global variance}}, \quad (5)$$

where \mathcal{O} swallows all constants (including L), and $F = f(\mathbf{x}^0) - f(\mathbf{x}^*)$, $\bar{\mathbf{x}}^R = \frac{1}{R} \sum_{r=0}^{R-1} \mathbf{x}^r$ is the averaged global model over the R rounds.

The upper bound of $\mathbb{E}[\|\nabla f(\bar{\mathbf{x}}^R)\|^2]$ consists of three types of terms: (i) initialization error, (ii) client drift error, caused by the client drift (see Lemma 4 in Appendix C.2), (iii) global variance. We can see that the result demonstrates the relationships between convergence and factors such as the number of clients, the data heterogeneity, the learning rate and the local update steps. According to the result, a large η means higher rate that the initialization error decreases at but causes large client drift error and global variance. Next, we discuss the convergence rate and the influence factors of SL in detail.

Convergence rate. By Corollary 1, for sufficiently large R , the convergence rate is determined by the initialization error and global variance (see Eq. (5)), resulting in a convergence rate of $\mathcal{O}(1/\sqrt{R})$, where R is the number of total training rounds. However, Theorem 1 has not incorporated the IID case even when $B = 1$ and $G = 0$.

Effect of data heterogeneity. According to Theorem 1, when on highly non-IID data (B and G are large), a small learning rate η is required for the convergence of SL (see the condition of Theorem 1). In addition, the client drift error increases. As a result, large data heterogeneity harms the convergence of SL, which is consistent with the previous study (Gao et al., 2020, 2021).

Effect of synchronization interval. By Eq. (4), as K increases, the initialization error decreases and the client drift error increases, which indicates that the optimal K exists. This means that we can improve the convergence by increasing local update steps when R is fixed. We can further obtain that larger data heterogeneity makes the optimal K smaller based on Eq. (4). This property is analogous to FL (McMahan et al., 2017).

More detailed analyses of these factors combined with the experiments are given in Section 5.2.

4.3 Comparison between FL and SL

In this section, we reproduce the convergence result of FL³ according to Wang et al. (2020) in our setting, and then compare the results of FL and SL to answer the second question “*In which setting will the SL performance outperform FL?*” theoretically.

We summarize the convergence results of FL (reproduced by Theorem 2 in Appendix C.3) and SL (Theorem 1) in Table 1. The convergence guarantee of FL in Table 1 is one of the best known convergence results for the non-convex functions of FL, which makes our comparison persuasive.

The constraint on the learning rate of SL is tougher than FL. The learning rate of SL has tougher constraints than FL (see the 3, 6-th rows of Table 1), which indicates SL is more sensitive to the heterogeneity of data. This is significant for the selection of the learning rate of SL in practice (see the comparison experiments).

Effective learning rate. We next focus on comparing FL and SL in terms of training rounds. Note that this comparison (running for the same R) is fair given the same total computation

³Assumptions 1, 2 and 3 are also adopted in FL. In addition, the global learning rate of FL is set to be 1 for comparison (Karimireddy et al., 2020; Wang et al., 2020).

Table 1: Comparison of convergence results between FL (Wang et al., 2020) and SL (Theorem 1) for non-convex functions. The convergence guarantee of FL is given in the 1-st row with $\tilde{\eta}_{\text{FL}} := K\eta$ and the convergence guarantee of SL is in the 4-th row with $\tilde{\eta}_{\text{SL}} := NK\eta$. The number of rounds required to reach ϵ accuracy is given in the 2-nd (FL) and 5-th (SL) rows. The constraints are given in the 3-rd (FL) and 6-th (SL) rows. Constants (including L) are omitted.

FL (Wang et al., 2020)	$\tilde{\eta}_{\text{FL}}: \mathcal{O}\left(\frac{F}{\tilde{\eta}_{\text{FL}}R}\right) + \mathcal{O}\left(\tilde{\eta}_{\text{FL}}^2 G^2 + \frac{\tilde{\eta}_{\text{FL}}^2 \sigma^2}{K}\right) + \mathcal{O}\left(\frac{\tilde{\eta}_{\text{FL}} \sigma^2}{NK}\right)$
	$R_\epsilon = \mathcal{O}\left(\frac{F^2}{\epsilon^2} + \frac{\sigma^4}{N^2 K^2 \epsilon^2} + \frac{KG^2 + \sigma^2}{K\epsilon}\right)$
	Constraint: $\eta \leq \mathcal{O}\left(\frac{1}{K\sqrt{2B^2+1}}\right)$
SL	$\tilde{\eta}_{\text{SL}}: \mathcal{O}\left(\frac{F}{\tilde{\eta}_{\text{SL}}R}\right) + \mathcal{O}\left(\tilde{\eta}_{\text{SL}}^2 G^2 + \frac{\tilde{\eta}_{\text{SL}}^2 \sigma^2}{K}\right) + \mathcal{O}\left(\frac{\tilde{\eta}_{\text{SL}} \sigma^2}{K}\right)$
	$R_\epsilon = \mathcal{O}\left(\frac{F^2}{\epsilon^2} + \frac{\sigma^4}{K^2 \epsilon^2} + \frac{KG^2 + \sigma^2}{K\epsilon}\right)$
	Constraint: $\eta \leq \mathcal{O}\left(\frac{1}{NK\sqrt{2B^2+1}}\right)$

cost (including the computation cost on client-side and server-side). Observe that the convergence guarantees and constraints seem very alike if choosing $\eta_{\text{FL}} = N\eta_{\text{SL}}$, where η_{FL} and η_{SL} denote the learning rate of FL and SL respectively. So we define the effective learning rate $\tilde{\eta}_{\text{FL}} := K\eta$ for FL and $\tilde{\eta}_{\text{SL}} := NK\eta$ for SL as Karimireddy et al. (2020); Wang et al. (2020) did. Note that the effective learning rates are unequal for FL and SL. As a result, we obtain the convergence guarantee of the effective learning rate version exhibited in the 1-st and 4-th rows in Table 1.

The guarantee of SL is worse than FL in terms of training rounds on non-IID data. To make a comparison, we need to choose appropriate learning rate for both algorithms. Considering $\tilde{\eta}_{\text{FL}}$ and $\tilde{\eta}_{\text{SL}}$ have the same constraint, we can choose $\tilde{\eta}_{\text{FL}} = \tilde{\eta}_{\text{SL}} = 1/\sqrt{R}$ for both bounds. Then we get (i) $\mathcal{O}\left(\frac{F}{\sqrt{R}} + \frac{KG^2 + \sigma^2}{KR} + \frac{\sigma^2}{NK\sqrt{R}}\right)$ of FL and (ii) $\mathcal{O}\left(\frac{F}{\sqrt{R}} + \frac{KG^2 + \sigma^2}{KR} + \frac{\sigma^2}{K\sqrt{R}}\right)$ of SL after R rounds, and the round complexity R_ϵ shown in 2-nd and 5-th rows in Table 1. Then note that for sufficiently large R , R_ϵ is determined by the first and the second term (see the 2-nd and 5-th rows). In particular, the only difference in the complexity appears in the second term (we have marked it with pink), which indicates that the guarantee of SL is worse than FL in terms of training rounds. However, the gap is not obvious when K is small. As a consequence, to make a more detailed comparison, we have conducted adequate experiments in Section 5.3.

5 Experiments

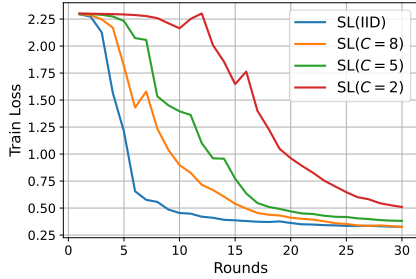
The experimental environment is ideal (without the communication and computation restrictions), nevertheless, is enough to examine our convergence theory. The convergence rate is evaluated in terms of the training rounds. We demonstrate the detailed experimental setup in Section 5.1, evaluate the effect of the factors on the performance of SL in Section 5.2, and compare FL and SL in cross-device settings in Section 5.3. More experimental details are in Appendix D.

5.1 Experimental Setup

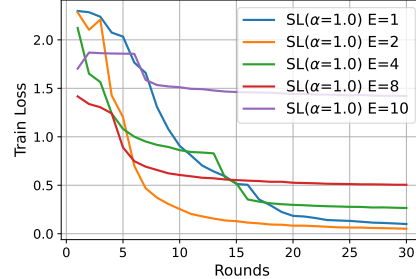
Datasets and models. We adopt the following setups: (i) training LeNet-5 (LeCun et al., 1998) on the MNIST dataset (LeCun et al., 1998); (ii) training LeNet-5 on the Fashion-MNIST dataset (Xiao et al., 2017); (iii) training VGG-11 (Simonyan and Zisserman, 2014) on the CIFAR-10 dataset (Krizhevsky et al., 2009). For SL, the LeNet-5 is split after the second 2D MaxPool layer, with 6% of the entire model size retained in the client; the VGG-11 is split after the third 2D MaxPool layer, with 10% of the entire model size at the client. Ideally, the split layer position has no effect on the performance of SL (Wang et al., 2022).

Data distribution. For the non-IID setting, we adopt two mechanisms to generate non-IID data: (i) using a Dirichlet distribution $\text{Dir}(\alpha)$, where a smaller α indicates higher data heterogeneity (Hsu et al., 2019; Zhu et al., 2021); (ii) using a similar mechanism like (McMahan et al., 2017; Zhao et al., 2018), e.g., one distribution in which most clients only contain samples from 2 (5) classes, denoted as $C = 2$ (5). Note that the data distribution generated by the first mechanism is unbalanced and the second is balanced. We will use “ α ” and “ C ” to represent the different data distributions in the following experiments.

5.2 Experimental Results of SL



(a) Effect of data heterogeneity



(b) Effect of synchronization interval

Figure 3: Results of SL on MNIST dataset.

In this section, we study the effects of data heterogeneity and synchronization interval using the MNIST dataset. The training samples are assigned to 10 clients. For data heterogeneity, we use four distributions: IID, $C = 8, 5, 2$. For synchronization interval, we use five settings, $E = 1, 2, 4, 8, 10$ over $\text{Dir}_{10}(1.0)$ distribution. E is the local epochs (McMahan et al., 2017), which satisfies $\tau_i = En_i/b$, where b is the mini-batch size. So E can measure the value of synchronization interval with n_i and b fixed. The results on Fashion-MNIST and CIFAR-10 are deferred to Appendix D.1.

Effect of data heterogeneity. As shown in Figure 3a, the training loss curve of IID distribution is the lowest and most stable. When the data heterogeneity increases (C decreases from 8 to 2), SL shows worse performance. The phenomenon is in accordance with our analysis that large data heterogeneity harms the convergence of SL in Section 4.2.

Effect of synchronization interval. Figure 3b shows the training loss in terms of training rounds R . SL shows the best performance when $E = 2$. This verifies that optimal interval exists and choosing suitable interval can improve the convergence. Besides, over-large interval can even harm the convergence rate (see curves $E = 8$ and $E = 10$).

5.3 Empirical Comparison between FL and SL

We have compared FL and SL theoretically in Section 4.2. The question arises that *how about the learning performance of SL in practice compared to FL?* In the previous work, the same learning rates are used to evaluate the performances of SL and FL (Gao et al., 2020, 2021). However, theoretical analyses in Section 4.2 show that the appropriate learning rate for SL may deviate from that of FL. Thus, we evaluate the performance of SL and FL with different learning rates for fair comparison. The learning rates are selected from $\{0.0005, 0.001, 0.005, 0.01, 0.05, 0.1\}$. To evaluate the effect of model synchronization interval on the performance comparison of FL and SL, we adopt two settings: $E = 1$ and $E = 10$. We run 1000 rounds of training on MNIST, Fashion-MNIST and 4000 rounds on CIFAR-10 dataset when $E = 1$; run 100 rounds of training on MNIST, Fashion-MNIST and 400 rounds on CIFAR-10 dataset when $E = 10$. The average top-1 test accuracy over the last 10% rounds are shown in Table 2, e.g., the average accuracy over the last 400 rounds of the total 4000 rounds on CIFAR-10 when $E = 1$. The full results are provided in Appendix D.2.

Table 2: Performance comparison between FL and SL in cross-device settings. The “best” test accuracy (%) is in the “Best” accuracy (lr) column (the “best” learning rate is in the parenthesis) and the “threshold” learning rate in the “Threshold” lr column. Note that $>\#$ means that the “threshold” learning rate is larger than $\#$. The higher “best” accuracy between FL and SL is marked in bold (excluding the results whose difference is within 1%).

	Dataset	Distribution	$E = 1$				$E = 10$			
			“Best” accuracy (lr)		“Threshold” lr		“Best” accuracy (lr)		“Threshold” lr	
			FL	SL	FL	SL	FL	SL	FL	SL
1	MNIST	IID	99.0 (0.05)	98.9 (0.005)	> 0.1	0.05	97.9 (0.01)	97.6 (0.005)	0.1	0.05
2		$\alpha = 5.0$	99.1 (0.05)	98.9 (0.01)	> 0.1	0.05	98.0 (0.01)	97.8 (0.001)	0.05	0.01
3		$\alpha = 0.5$	98.9 (0.05)	98.8 (0.005)	> 0.1	0.05	97.9 (0.01)	97.9 (0.001)	0.05	0.005
4		$\alpha = 0.2$	98.7 (0.05)	98.8 (0.005)	0.1	0.05	96.8 (0.01)	96.8 (0.001)	0.05	0.01
5		$C = 5$	99.0 (0.05)	98.9 (0.005)	> 0.1	0.05	98.0 (0.01)	98.0 (0.001)	0.05	0.01
6		$C = 2$	98.8 (0.05)	99.0 (0.01)	> 0.1	0.05	96.8 (0.005)	97.1 (0.001)	0.05	0.005
7	Fashion-MNIST	IID	88.1 (0.05)	88.4 (0.005)	> 0.1	0.1	85.0 (0.01)	84.0 (0.001)	0.1	0.05
8		$\alpha = 5.0$	88.2 (0.05)	88.8 (0.005)	> 0.1	0.1	84.5 (0.01)	83.2 (0.0005)	0.05	0.05
9		$\alpha = 0.5$	86.7 (0.05)	87.6 (0.005)	> 0.1	0.1	83.8 (0.01)	79.2 (0.001)	0.05	0.01
10		$\alpha = 0.2$	83.5 (0.01)	85.9 (0.005)	0.1	0.05	80.4 (0.01)	79.0 (0.0005)	0.05	0.01
11		$C = 5$	87.5 (0.05)	88.1 (0.01)	> 0.1	0.05	82.7 (0.01)	80.1 (0.001)	0.1	0.05
12		$C = 2$	83.0 (0.1)	87.3 (0.005)	> 0.1	0.05	75.9 (0.01)	72.3 (0.001)	0.1	0.005
13	CIFAR-10	IID	86.4 (0.05)	87.0 (0.005)	0.1	0.05	77.7 (0.01)	83.7 (0.001)	0.05	0.01
14		$\alpha = 5.0$	86.1 (0.05)	87.0 (0.005)	0.1	0.05	77.6 (0.005)	82.7 (0.001)	0.05	0.005
15		$\alpha = 0.5$	84.1 (0.01)	85.5 (0.005)	0.05	0.01	71.8 (0.01)	76.9 (0.001)	0.05	0.005
16		$\alpha = 0.2$	80.5 (0.01)	83.5 (0.001)	0.05	0.01	66.9 (0.01)	65.0 (0.0005)	0.05	0.001
17		$C = 5$	85.5 (0.05)	86.5 (0.005)	0.1	0.05	74.2 (0.01)	78.9 (0.001)	0.05	0.005
18		$C = 2$	80.0 (0.05)	84.7 (0.005)	0.1	0.05	61.6 (0.01)	58.7 (0.0005)	0.05	0.001

Cross-device setting. We compare the performance of FL and SL in cross-device settings, where the client number is enormous and the local dataset size is small. Specifically, (i) MNIST: the training data is split into 1000 clients; (ii) Fashion-MNIST: the training data is split into 1000 clients; (iii) CIFAR-10: the training data is split into 500 clients. The number of samples per client depends on the data distribution, e.g., 60 (MNIST), 60 (Fashion-MNIST) and 100 (CIFAR-10) samples per client in the second partition mechanism. The mini-batch size is 10 for all setups under the consideration of low computation power of IoT devices. The original test sets are used

to evaluate the generalization performance of the global model (test accuracy) after each training round.

The best and threshold learning rate of SL is smaller than FL. We refer to the learning rate making the best test accuracy and minimal learning rate making the training die as the best learning rate and the threshold learning rate. According to our theory, the tougher constraint indicates the smaller threshold learning rate of SL and the math property of Eq. (4) indicates a smaller best learning rate. To verify this point, we use the “best” learning rate, which makes the “best” test accuracy among the learning rates we choose, to substitute the actual best learning rate. The “threshold” learning rate is defined alike. As shown in Table 2, the “best” and “threshold” learning rates of SL are smaller than FL, especially on highly non-IID data (e.g., $\alpha = 0.2$). Furthermore, we note that the “best” and “threshold” learning rate turn small as the heterogeneity of data becomes large, which is also in accordance with our theory.

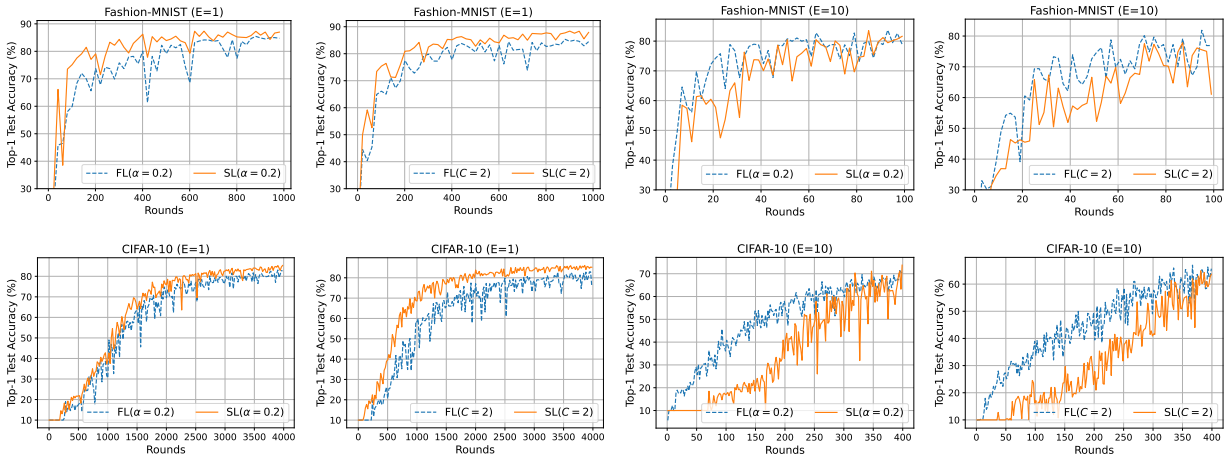


Figure 4: Top-1 test accuracy of FL and SL on non-IID data in terms of training rounds. We draw some results of Fashion-MNIST and CIFAR-10 from Table 2. (i) Top row: The results on Fashion-MNIST, from left to right, $E = 1$, $\alpha = 0.2$; $E = 1$, $C = 2$; $E = 10$, $\alpha = 0.2$; $E = 10$, $C = 2$. (ii) Bottom row: The results on CIFAR-10, from left to right, $E = 1$, $\alpha = 0.2$; $E = 1$, $C = 2$; $E = 10$, $\alpha = 0.2$; $E = 10$, $C = 2$.

Performance comparison on non-IID data. Our theory proves that the guarantee of SL is worse than FL in terms of training rounds, especially when the synchronization interval is large. We see that FL achieves better generalization performance and faster convergence speed than SL when the interval is large from the right four plots in Figure 4. Moreover, almost all the “best” test accuracy of FL on highly non-IID data (i.e., $\alpha = 0.2$ and $C = 2$) beats that of SL when $E = 10$ in Table 2.

However, as shown in the left four plots of Figure 4, SL has a better performance than FL when the interval is small. We can also obtain it from the $E = 1$ column and even in some cases (e.g., $\alpha = 0.5$ and $C = 5$ on CIFAR-10) when $E = 10$ in Table 2.

6 Conclusion

In this work, we have derived the convergence guarantee of SL for non-convex objectives on non-IID data. The results reveal that the convergence of SL is affected by the factors such as data heterogeneity and synchronization interval. Furthermore, we have compared the convergence guarantee

of SL against FL, showing that (i) the best and threshold learning rate of SL is smaller than FL (ii) and the guarantee of SL is worse than FL in terms of training rounds on non-IID data. Adequate experiments in the cross-device settings have been carried to verify our theory. In addition, we find that the performance of SL can be better than FL when the synchronization interval is small on non-IID data empirically. We believe that this work can bridge the gap between FL and SL, provide deep understanding of both approaches and guide the application deployment in real world.

References

- Ahmad Ajalloeian and Sebastian U Stich. On the convergence of sgd with biased gradients. *arXiv preprint arXiv:2008.00051*, 2020.
- Eugene Belilovsky, Michael Eickenberg, and Edouard Oyallon. Decoupled greedy learning of CNNs. In *International Conference on Machine Learning*, pages 736–745. PMLR, 2020.
- Qiang Duan, Shijing Hu, Ruijun Deng, and Zhihui Lu. Combined federated and split learning in edge computing for ubiquitous intelligence in internet of things: State-of-the-art and future directions. *Sensors*, 22(16):5983, 2022.
- Yansong Gao, Minki Kim, Sharif Abuadbba, Yeonjae Kim, Chandra Thapa, Kyuyeon Kim, Seyit A Camtepe, Hyounghick Kim, and Surya Nepal. End-to-end evaluation of federated learning and split learning for internet of things. *arXiv preprint arXiv:2003.13376*, 2020.
- Yansong Gao, Minki Kim, Chandra Thapa, Sharif Abuadbba, Zhi Zhang, Seyit Camtepe, Hyounghick Kim, and Surya Nepal. Evaluation and optimization of distributed machine learning techniques for internet of things. *IEEE Transactions on Computers*, 2021.
- Manish Gawali, Shriya Suryavanshi, Harshit Madaan, Ashrika Gaikwad, Bhanu Prakash KN, Viraj Kulkarni, Aniruddha Pant, et al. Comparison of privacy-preserving distributed deep learning methods in healthcare. *arXiv preprint arXiv:2012.12591*, 2020.
- Otkrist Gupta and Ramesh Raskar. Distributed learning of deep neural network over multiple agents. *Journal of Network and Computer Applications*, 116:1–8, 2018.
- Dong-Jun Han, Hasnain Irshad Bhatti, Jungmoon Lee, and Jaekyun Moon. Accelerating federated learning with split learning on locally generated losses. In *ICML 2021 Workshop on Federated Learning for User Privacy and Data Confidentiality. ICML Board*, 2021.
- Chaoyang He, Murali Annavaram, and Salman Avestimehr. Group knowledge transfer: Federated learning of large cnns at the edge. *Advances in Neural Information Processing Systems*, 33: 14068–14080, 2020.
- Tzu-Ming Harry Hsu, Hang Qi, and Matthew Brown. Measuring the effects of non-identical data distribution for federated visual classification. *arXiv preprint arXiv:1909.06335*, 2019.
- Peter Kairouz, H Brendan McMahan, Brendan Avent, Aurélien Bellet, Mehdi Bennis, Arjun Nitin Bhagoji, Kallista Bonawitz, Zachary Charles, Graham Cormode, Rachel Cummings, et al. Advances and open problems in federated learning. *Foundations and Trends® in Machine Learning*, 14(1–2):1–210, 2021.
- Sai Praneeth Karimireddy, Satyen Kale, Mehryar Mohri, Sashank Reddi, Sebastian Stich, and Ananda Theertha Suresh. Scaffold: Stochastic controlled averaging for federated learning. In *International Conference on Machine Learning*, pages 5132–5143. PMLR, 2020.
- Ahmed Khaled, Konstantin Mishchenko, and Peter Richtárik. Tighter theory for local sgd on identical and heterogeneous data. In *International Conference on Artificial Intelligence and Statistics*, pages 4519–4529. PMLR, 2020.
- Alex Krizhevsky et al. Learning multiple layers of features from tiny images. *Technical report*, 2009.

- Yann LeCun, Léon Bottou, Yoshua Bengio, and Patrick Haffner. Gradient-based learning applied to document recognition. *Proceedings of the IEEE*, 86(11):2278–2324, 1998.
- Qinbin Li, Yiqun Diao, Quan Chen, and Bingsheng He. Federated learning on non-iid data silos: An experimental study. In *2022 IEEE 38th International Conference on Data Engineering (ICDE)*, pages 965–978. IEEE, 2022.
- Tian Li, Anit Kumar Sahu, Manzil Zaheer, Maziar Sanjabi, Ameet Talwalkar, and Virginia Smith. Federated optimization in heterogeneous networks. *Proceedings of Machine Learning and Systems*, 2:429–450, 2020.
- Xiang Li, Kaixuan Huang, Wenhao Yang, Shusen Wang, and Zhihua Zhang. On the convergence of fedavg on non-iid data. *arXiv preprint arXiv:1907.02189*, 2019.
- Xiangru Lian, Ce Zhang, Huan Zhang, Cho-Jui Hsieh, Wei Zhang, and Ji Liu. Can decentralized algorithms outperform centralized algorithms? a case study for decentralized parallel stochastic gradient descent. *Advances in Neural Information Processing Systems*, 30, 2017.
- Brendan McMahan, Eider Moore, Daniel Ramage, Seth Hampson, and Blaise Aguera y Arcas. Communication-efficient learning of deep networks from decentralized data. In *Artificial intelligence and statistics*, pages 1273–1282. PMLR, 2017.
- Jihong Park, Sumudu Samarakoon, Anis Elgabri, Joongheon Kim, Mehdi Bennis, Seong-Lyun Kim, and Mérouane Debbah. Communication-efficient and distributed learning over wireless networks: Principles and applications. *Proceedings of the IEEE*, 109(5):796–819, 2021.
- Karen Simonyan and Andrew Zisserman. Very deep convolutional networks for large-scale image recognition. *arXiv preprint arXiv:1409.1556*, 2014.
- Abhishek Singh, Praneeth Vepakomma, Otkrist Gupta, and Ramesh Raskar. Detailed comparison of communication efficiency of split learning and federated learning. *arXiv preprint arXiv:1909.09145*, 2019.
- Sebastian Urban Stich. Local SGD converges fast and communicates little. *International Conference on Learning Representations (ICLR)*, page arXiv:1805.09767, 2019. URL <https://arxiv.org/abs/1805.09767>.
- Chandra Thapa, Mahawaga Arachchige Pathum Chamikara, Seyit Camtepe, and Lichao Sun. Splitfed: When federated learning meets split learning. *arXiv preprint arXiv:2004.12088*, 2020.
- Chandra Thapa, Mahawaga Arachchige Pathum Chamikara, and Seyit A Camtepe. Advancements of federated learning towards privacy preservation: from federated learning to split learning. In *Federated Learning Systems*, pages 79–109. Springer, 2021.
- Praneeth Vepakomma, Otkrist Gupta, Tristan Swedish, and Ramesh Raskar. Split learning for health: Distributed deep learning without sharing raw patient data. *arXiv preprint arXiv:1812.00564*, 2018.
- Jianyu Wang, Qinghua Liu, Hao Liang, Gauri Joshi, and H Vincent Poor. Tackling the objective inconsistency problem in heterogeneous federated optimization. *Advances in neural information processing systems*, 33:7611–7623, 2020.

- Jianyu Wang, Hang Qi, Ankit Singh Rawat, Sashank Reddi, Sagar Waghmare, Felix X Yu, and Gauri Joshi. Fedlite: A scalable approach for federated learning on resource-constrained clients. *arXiv preprint arXiv:2201.11865*, 2022.
- Blake Woodworth, Kumar Kshitij Patel, Sebastian Stich, Zhen Dai, Brian Bullins, Brendan McMahan, Ohad Shamir, and Nathan Srebro. Is local sgd better than minibatch sgd? In *International Conference on Machine Learning*, pages 10334–10343. PMLR, 2020a.
- Blake E Woodworth, Kumar Kshitij Patel, and Nati Srebro. Minibatch vs local sgd for heterogeneous distributed learning. *Advances in Neural Information Processing Systems*, 33:6281–6292, 2020b.
- Han Xiao, Kashif Rasul, and Roland Vollgraf. Fashion-mnist: a novel image dataset for benchmarking machine learning algorithms. *arXiv preprint arXiv:1708.07747*, 2017.
- Riccardo Zaccone, Andrea Rizzardi, Debora Caldarola, Marco Ciccone, and Barbara Caputo. Speeding up heterogeneous federated learning with sequentially trained superclients. *arXiv preprint arXiv:2201.10899*, 2022.
- Yue Zhao, Meng Li, Liangzhen Lai, Naveen Suda, Damon Civin, and Vikas Chandra. Federated learning with non-iid data. *arXiv preprint arXiv:1806.00582*, 2018.
- Fan Zhou and Guojing Cong. On the convergence properties of a k -step averaging stochastic gradient descent algorithm for nonconvex optimization. *arXiv preprint arXiv:1708.01012*, 2017.
- Zhi Zhou, Xu Chen, En Li, Liekang Zeng, Ke Luo, and Junshan Zhang. Edge intelligence: Paving the last mile of artificial intelligence with edge computing. *Proceedings of the IEEE*, 107(8): 1738–1762, 2019.
- Zhuangdi Zhu, Junyuan Hong, and Jiayu Zhou. Data-free knowledge distillation for heterogeneous federated learning. In *International Conference on Machine Learning*, pages 12878–12889. PMLR, 2021.

APPENDIX

A	Additional related work	16
B	Summary of theories	17
C	Proof of results	17
C.1	Basic technical lemmas and Notations	17
C.2	Proof of Theorem 1	22
C.3	Proof of Theorem 2	24
C.4	Proof of Theorem 3	24
D	More experimental details	28
D.1	More results of SL	28
D.2	More comparisons between FL and SL in cross-device setting	28

A Additional related work

Variants of SL. SL is deemed as a promising paradigm for distributed model training at resource-constrained devices, given its computational efficiency on the client side. Most existing works focus on reducing the training delay arising from the relay-based training manner in the multi-user scenario. **SplitFed** (Thapa et al., 2020) is one popular model parallel algorithm that combines the strengths of FL and SL, where each client has one corresponding instance of server-side model in the *main server* to form a pair. Each pair constitutes a complete model and conducts the local update in parallel. After each training round, the *fed server* collects and aggregates on the client-side local updates. The aggregated client-side model will be disseminated to all the clients before next round. The *main server* does the same operations to the instances of the server-side model. However, in **SplitFed**, the *main server* is required for great computing power to support the multiple instances of server-side model. To address this issue, Thapa et al. (2020) proposed **SplitFedv2**. The only change in **SplitFedv2** is that only one server-side model in *main server*. So the server-side model has to process the activations (or smashed data) of the client-side model in sequence. The model gets updated in every single forward-backward propagation, which means that the server-side model makes more updates than the client-side model. The main point of **SplitFedv3** (Gawali et al., 2020) is substituting alternative client training with alternative the mini-batch training. In vanilla SL, the local model makes one or more training passes over the local dataset (alternative client training). This may cause “catastrophic forgetting” issue (Gawali et al., 2020; Duan et al., 2022). So **SplitFedv3** propose to use alternate mini-batch training, where a client updates its client-side model on one mini-batch, after which the client next in order takes over (Gawali et al., 2020), to mitigate the issue. **SFLG** (Gao et al., 2021) is one generalized variants of **SplitFed**. The clients are allocated to multiple groups. There is one server in each group. The training inside the group is identical to **SplitFedv2**. Then the server-side “global” models per group are aggregated (e.g., weighted averaging) to obtain the server-side global model of all groups. **FedSeq** (Zaccone et al., 2022) is the same as **SFLG** except that the training inside the group is identical to vanilla SL. More variants can be found in Thapa et al. (2021); Duan et al. (2022).

Convergence analysis of SL. The convergence analysis of SL is identical to standard Minibatch-SGD on IID data (Wang et al., 2022; Park et al., 2021), so some convergence properties of Minibatch-SGD is applied to SL too. The algorithm in Han et al. (2021) reduces the latency and downlink communication on **SplitFed** by adding auxiliary networks at client-side to generate the local loss for model updating. Their convergence analysis combines the analysis of Belilovsky et al. (2020) and FedAvg. Wang et al. (2022) proposed **FedLite** to reduce the uplink communication overhead by compressing activations with product quantization and provided the convergence analysis of **FedLite**. However, their convergence recovers that of Minibatch-SGD when there is no quantization. SGD with biased gradients (Ajallooeian and Stich, 2020) is also related. However, it only converges to a neighborhood of the solution. Furthermore, we find that Woodworth et al. (2020a,b) compared the convergence of distributed Minibatch-SGD and local SGD under homogeneous and heterogeneous settings. To differentiate our work, we show how Minibatch-SGD, FL and SL operate in Table 3. They all aim to optimize one global objective, $\min f(\mathbf{x}) = \frac{1}{N} \sum_{i=1}^N f_i(\mathbf{x})$ for N clients, each of which has its own local dataset \mathcal{D}_i . Here $f_i(\mathbf{x}) := \mathbb{E}_{\xi_i \sim \mathcal{D}_i} [f_i(\mathbf{x}; \xi_i)]$ is the local objective function of client i . The learning rate is denoted as η . The global model parameter is denoted as \mathbf{x}^r in the r -th round. In particular, we use $\mathbf{x}_i^{(r,k)}$ to denote the local model parameter of client i after k -th local update in the r -th round for FL and SL. We use $\nabla f_i(\mathbf{x}; \xi)$ to represent the stochastic gradient of f_i computed by the parameter \mathbf{x} and the data sample ξ . Note that we assume that the number of local update steps of all clients in FL and SL is K . We can see that (i) there is no local

update and each client computes K stochastic gradients at the same point \mathbf{x}^r in Minibatch SGD; (ii) clients in FL make local training in parallel, while clients in SL make local training in sequence.

Table 3: The update rules of Minibatch SGD, FL (Local SGD) and SL.

Algorithm	Global model update	Local update of client i
Minibatch SGD	$\mathbf{x}^{r+1} = \mathbf{x}^r - \eta \frac{1}{NK} \sum_{i=1}^N \sum_{k=0}^{K-1} \nabla f_i(\mathbf{x}^r; \xi_i^{(r,k)})$	-
Local SGD (or FL)	$\mathbf{x}^{r+1} = \mathbf{x}^r - \eta \frac{1}{N} \sum_{i=1}^N \sum_{k=0}^{K-1} \nabla f_i(\mathbf{x}_i^{(r,k)}; \xi_i^{(r,k)})$	Initialize: $\mathbf{x}_i^{(r,0)} = \mathbf{x}^r$ Update: $\mathbf{x}_i^{(r,k+1)} = \mathbf{x}_i^{(r,k)} - \eta \nabla f_i(\mathbf{x}_i^{(r,k)}; \xi_i^{(r,k)})$
SL	$\mathbf{x}^{r+1} = \mathbf{x}^r - \eta \sum_{i=1}^N \sum_{k=0}^{K-1} \nabla f_i(\mathbf{x}_i^{(r,k)}; \xi_i^{(r,k)})$	Initialize: $\mathbf{x}_i^{(r,0)} = \mathbf{x}_{i-1}^{(r,K)}$ Update: $\mathbf{x}_i^{(r,k+1)} = \mathbf{x}_i^{(r,k)} - \eta \nabla f_i(\mathbf{x}_i^{(r,k)}; \xi_i^{(r,k)})$

B Summary of theories

Table 4 summarizes the notations.

There are two methods to give the convergence of SL: (i) bounding the progress of all clients in one round; (ii) bounding the progress of one client in one round. The second method can be given based on the techniques of FL (Khaled et al., 2020; Karimireddy et al., 2020; Wang et al., 2020) directly. However, it only converges to a neighborhood around the stationary point of the global function. This case is similar to the biased SGD (Ajalloeian and Stich, 2020). It is intuitive to get the conclusion since the local stochastic gradient $\nabla f_i(\mathbf{x}; \xi_i)$ ($\xi_i \sim \mathcal{D}_i$) generated by local data of any client i is a biased gradient estimator of the global gradient $\nabla f(\mathbf{x})$ of the global function. For the first method — bounding the progress of all clients in one round, our main contribution, shows that SL can converge to the stationary point of the global function. The main theories are summarized in Table 5.

C Proof of results

C.1 Basic technical lemmas and Notations

Lemma 1. $\mathbf{x}_1, \dots, \mathbf{x}_N$ are N vectors, then

$$\|\mathbf{x}_i + \mathbf{x}_j\|^2 \leq 2\|\mathbf{x}_i\|^2 + 2\|\mathbf{x}_j\|^2 \quad (6)$$

$$\|\mathbf{x}_i + \mathbf{x}_j\|^2 \leq (1+a)\|\mathbf{x}_i\|^2 + (1+\frac{1}{a})\|\mathbf{x}_j\|^2 \quad \text{for any } a > 0, \quad (7)$$

$$\left\| \sum_{i=1}^N \mathbf{x}_i \right\|^2 \leq N \sum_{i=1}^N \|\mathbf{x}_i\|^2. \quad (8)$$

Lemma 2 (Jensen’s inequality). For any convex function f and any vectors $\mathbf{x}_1, \dots, \mathbf{x}_N$ we have

$$f\left(\frac{1}{N} \sum_{i=1}^N \mathbf{x}_i\right) \leq \frac{1}{N} \sum_{i=1}^N f(\mathbf{x}_i). \quad (9)$$

Table 4: Summary of notations appearing in the paper.

Symbol	Description
R, r	Number, index of training rounds
N, i	Number, index of clients
τ_i	Number of local update steps (or synchronization interval) of client i . We assume that $\tau_i = \tau_j = K$ for $i \neq j$ in Theorem 1.
K, k	Number, index of local update steps;
\mathcal{S}, S	Subset of clients sampled for training every round and its size
n, n_i	Sizes of the overall dataset \mathcal{D} and local dataset \mathcal{D}_i at client i
E	Local epochs (see Section 5.2); number of training passes each client makes over its local dataset
b	Mini-batch size
η	The learning rate
L	L -smoothness constant in Assumption 1
σ	Upper bound on variance of stochastic gradient at each client (see Assumption 2)
B, G	See Assumption 3
α, C	They are used to denote different distributions by the two mechanisms generating non-IID data respectively (see Section 5.1)
$\mathbf{x}, \mathbf{x}_c, \mathbf{x}_s$	The full, client-side, server-side model
\mathbf{x}^r	The full global model (parameters) in the r -th round
$\mathbf{x}_i^{(r,k)}$	The full local model (parameters) after the k -th local update on the local dataset \mathcal{D}_i in the r -th round
$\mathbf{g}_i(\mathbf{x}_i^{(r,k)})$	$\mathbf{g}_i(\mathbf{x}_i^{(r,k)}) := \nabla f_i(\mathbf{x}_i^{(r,k)}; \xi_i^{(r,k)})$, stochastic gradients of f_i on the model parameter $\mathbf{x}_i^{(r,k)}$ and mini-batch $\xi_i^{(r,k)}$ sampled randomly from \mathcal{D}_i

As a special case with $f(x) = \|x\|^2$, we obtain

$$\left\| \frac{1}{N} \sum_{i=1}^N \mathbf{x}_i \right\|^2 \leq \frac{1}{N} \sum_{i=1}^N \|\mathbf{x}_i\|^2. \quad (10)$$

Lemma 3. Suppose $\{A_k\}_{k=1}^T$ is a sequence of random matrices and $\mathbb{E}[A_k | A_{k-1}, A_{k-2}, \dots, A_1] = \mathbf{0}, \forall k$. Then,

$$\mathbb{E} \left[\left\| \sum_{k=1}^T A_k \right\|_F^2 \right] = \sum_{k=1}^T \mathbb{E} \left[\|A_k\|_F^2 \right]. \quad (11)$$

Table 5: Summary of theories for SL. $\tilde{\eta}$ is the effective learning rate defined in Section 4.3. $\tilde{\eta}$ in “progress of all clients in one round” is defined as $NK\eta$ while $\tilde{\eta}$ in “progress of one client in one round” is defined as $K\eta$. And $F := f(\mathbf{x}^0) - f(\mathbf{x}^*)$.

Outline	Theory
Progress of all clients in one round ($\tilde{\eta} = NK\eta$), Assumptions 1, 2, 3	
$\mathbb{E}[\ \nabla f(\mathbf{x}^r)\ ^2] \leq \mathcal{O}\left(\frac{f(\mathbf{x}^r) - f(\mathbf{x}^{r+1})}{\tilde{\eta}}\right) + \mathcal{O}\left(\tilde{\eta}^2 G^2 + \frac{\tilde{\eta}^2 \sigma^2}{K}\right) + \mathcal{O}\left(\frac{\tilde{\eta} \sigma^2}{K}\right)$	Thm. 1
$\frac{1}{R} \sum_{r=0}^{R-1} \mathbb{E}[\ \nabla f(\mathbf{x}^r)\ ^2] \leq \mathcal{O}\left(\frac{F}{\tilde{\eta} R}\right) + \mathcal{O}\left(\tilde{\eta}^2 G^2 + \frac{\tilde{\eta}^2 \sigma^2}{K}\right) + \mathcal{O}\left(\frac{\tilde{\eta} \sigma^2}{K}\right)$	Thm. 1
$\frac{1}{R} \sum_{r=0}^{R-1} \mathbb{E}[\ \nabla f(\mathbf{x}^r)\ ^2] \leq \mathcal{O}\left(\frac{F}{\sqrt{R}}\right) + \mathcal{O}\left(\frac{KG^2 + \sigma^2}{KR}\right) + \mathcal{O}\left(\frac{\sigma^2}{K\sqrt{R}}\right)$	Cor. 1
Progress of one client in one round ($\tilde{\eta} = K\eta$, Assumptions 1, 2, 4)	
$\mathbb{E}[\ \nabla f(\mathbf{x}_i^{(r,0)})\ ^2] \leq \mathcal{O}\left(\frac{f(\mathbf{x}_i^{(r,0)}) - f(\mathbf{x}_{i+1}^{(r,0)})}{\tilde{\eta}}\right) + \mathcal{O}\left(\tilde{\eta}^2 G^2 + \frac{\tilde{\eta}^2 \sigma^2}{K}\right) + \mathcal{O}\left(\frac{\tilde{\eta} \sigma^2}{K}\right) + \mathcal{O}(G^2)$	Thm. 3
$\frac{1}{NR} \sum_{r=0}^{R-1} \sum_{i=1}^N \mathbb{E}[\ \nabla f(\mathbf{x}_i^{(r,0)})\ ^2] \leq \mathcal{O}\left(\frac{F}{\tilde{\eta} NR}\right) + \mathcal{O}\left(\tilde{\eta}^2 G^2 + \frac{\tilde{\eta}^2 \sigma^2}{K}\right) + \mathcal{O}\left(\frac{\tilde{\eta} \sigma^2}{K}\right) + \mathcal{O}(G^2)$	Thm. 3

Proof. This is the Lemma 2 of Wang et al. (2020).

$$\mathbb{E} \left[\left\| \sum_{k=1}^T A_k \right\|_{\text{F}}^2 \right] = \sum_{k=1}^T \mathbb{E} [\|A_k\|_{\text{F}}^2] + \sum_{i=1}^T \sum_{j=1, j \neq i}^T \mathbb{E} [\text{Tr}\{A_i^\top A_j\}] \quad (12)$$

$$= \sum_{k=1}^T \mathbb{E} [\|A_k\|_{\text{F}}^2] + \sum_{i=1}^T \sum_{j=1, j \neq i}^T \text{Tr}\{\mathbb{E} [A_i^\top A_j]\} \quad (13)$$

Assume $i < j$. Then, using the law of total expectation,

$$\mathbb{E} [A_i^\top A_j] = \mathbb{E} [A_i^\top \mathbb{E}[A_j | A_i, \dots, A_1]] = \mathbf{0}. \quad (14)$$

□

Lemma 4 (Bounded Drift). *For any learning rate satisfying $\eta \leq \frac{1}{2NKL}$, the client drift caused by local updates is bounded, as given by:*

$$\sum_{i=1}^N \sum_{k=0}^{K-1} \mathbb{E} [\|\mathbf{x}_i^{(r,k)} - \mathbf{x}^r\|^2] \leq \frac{2N^3 K^2 \eta^2 \sigma^2 + 4N^3 K^3 \eta^2 (B^2 \|\nabla f(\mathbf{x}^r)\|^2 + G^2)}{1 - 4N^2 K^2 \eta^2 L^2} \quad (15)$$

Proof. This proof is based on the proof of Theorem 1 (Convergence of Surrogate Objective) of

Wang et al. (2020). Considering

$$\mathbf{x}_i^{(r,k)} - \mathbf{x}^r = \mathbf{x}_i^{(r,k)} - \mathbf{x}_i^{(r,0)} + \mathbf{x}_i^{(r,0)} - \mathbf{x}_{i-1}^{(r,0)} + \cdots + \mathbf{x}_2^{(r,0)} - \mathbf{x}_1^{(r,0)} \quad (16)$$

$$= -\eta \sum_{t=0}^{k-1} \mathbf{g}_i(\mathbf{x}_i^{(r,t)}) - \eta \sum_{s=1}^{i-1} \sum_{t=0}^{K-1} \mathbf{g}_s(\mathbf{x}_s^{(r,t)}), \quad (17)$$

we have

$$\begin{aligned} & \mathbb{E} \left[\left\| \mathbf{x}_i^{(r,k)} - \mathbf{x}^r \right\|^2 \right] \\ &= \eta^2 \mathbb{E} \left[\left\| \sum_{t=0}^{k-1} \mathbf{g}_i(\mathbf{x}_i^{(r,t)}) + \sum_{s=1}^{i-1} \sum_{t=0}^{K-1} \mathbf{g}_s(\mathbf{x}_s^{(r,t)}) \right\|^2 \right] \end{aligned} \quad (18)$$

$$\begin{aligned} &\leq 2\eta^2 \mathbb{E} \left[\left\| \sum_{t=0}^{k-1} [\mathbf{g}_i(\mathbf{x}_i^{(r,t)}) - \nabla f_i(\mathbf{x}_i^{(r,t)})] + \sum_{s=1}^{i-1} \sum_{t=0}^{K-1} [\mathbf{g}_s(\mathbf{x}_s^{(r,t)}) - \nabla f_s(\mathbf{x}_s^{(r,t)})] \right\|^2 \right] \\ &\quad + 2\eta^2 \mathbb{E} \left[\left\| \sum_{t=0}^{k-1} \nabla f_i(\mathbf{x}_i^{(r,t)}) + \sum_{s=1}^{i-1} \sum_{t=0}^{K-1} \nabla f_s(\mathbf{x}_s^{(r,t)}) \right\|^2 \right] \end{aligned} \quad (19)$$

$$\begin{aligned} &\stackrel{(8)}{\leq} 2i\eta^2 \mathbb{E} \left[\left\| \sum_{t=0}^{k-1} [\mathbf{g}_i(\mathbf{x}_i^{(r,t)}) - \nabla f_i(\mathbf{x}_i^{(r,t)})] \right\|^2 + \sum_{s=1}^{i-1} \left\| \sum_{t=0}^{K-1} [\mathbf{g}_s(\mathbf{x}_s^{(r,t)}) - \nabla f_s(\mathbf{x}_s^{(r,t)})] \right\|^2 \right] \\ &\quad + 2i\eta^2 \mathbb{E} \left[\left\| \sum_{t=0}^{k-1} \nabla f_i(\mathbf{x}_i^{(r,t)}) \right\|^2 + \sum_{s=1}^{i-1} \left\| \sum_{t=0}^{K-1} \nabla f_s(\mathbf{x}_s^{(r,t)}) \right\|^2 \right] \end{aligned} \quad (20)$$

Applying Lemma 3 to the first term and Jensen's Inequality to the second term on the right hand

side in Eq. (20) respectively, we get

$$\mathbb{E} \left[\left\| \mathbf{x}_i^{(r,k)} - \mathbf{x}^r \right\|^2 \right] \stackrel{\text{Asm. 2}}{\leq} 2i^2 K \eta^2 \sigma^2 + 2i K \eta^2 \sum_{s=1}^i \sum_{t=0}^{K-1} \mathbb{E} \left[\left\| \nabla f_s(\mathbf{x}_s^{(r,t)}) \right\|^2 \right] \quad (21)$$

$$\stackrel{(6)}{\leq} 2i^2 K \eta^2 \sigma^2 + 4i K \eta^2 \sum_{s=1}^i \sum_{t=0}^{K-1} \mathbb{E} \left[\left\| \nabla f_s(\mathbf{x}^r) \right\|^2 \right] + 4i K \eta^2 \sum_{s=1}^i \sum_{t=0}^{K-1} \mathbb{E} \left[\left\| \nabla f_s(\mathbf{x}_s^{(r,t)}) - \nabla f_s(\mathbf{x}^r) \right\|^2 \right] \quad (22)$$

$$\stackrel{\text{Asm. 1}}{\leq} 2i^2 K \eta^2 \sigma^2 + 4i K \eta^2 \sum_{s=1}^i \sum_{t=0}^{K-1} \mathbb{E} \left[\left\| \nabla f_s(\mathbf{x}^r) \right\|^2 \right] + 4i K \eta^2 L^2 \sum_{s=1}^i \sum_{t=0}^{K-1} \mathbb{E} \left[\left\| \mathbf{x}_s^{(r,t)} - \mathbf{x}^r \right\|^2 \right] \quad (23)$$

$$\leq 2i^2 K \eta^2 \sigma^2 + 4i K^2 \eta^2 \sum_{s=1}^N \mathbb{E} \left[\left\| \nabla f_s(\mathbf{x}^r) \right\|^2 \right] + \underbrace{4i K \eta^2 L^2 \sum_{s=1}^N \sum_{t=0}^{K-1} \mathbb{E} \left[\left\| \mathbf{x}_s^{(r,t)} - \mathbf{x}^r \right\|^2 \right]}_{\mathcal{E}} \quad (24)$$

Summing up $\mathbb{E} \left[\left\| \mathbf{x}_i^{(r,k)} - \mathbf{x}^r \right\|^2 \right]$ over i and k , we get

$$\sum_{i=1}^N \sum_{k=0}^{K-1} \mathbb{E} \left[\left\| \mathbf{x}_i^{(r,k)} - \mathbf{x}^r \right\|^2 \right] \leq 2K^2 \eta^2 \sigma^2 \sum_{i=1}^N i^2 + 4K^3 \eta^2 \sum_{s=1}^N \mathbb{E} \left[\left\| \nabla f_s(\mathbf{x}^r) \right\|^2 \right] \sum_{i=1}^N i + 4K^2 \eta^2 L^2 \mathcal{E} \sum_{i=1}^N i \quad (25)$$

$$\leq 2N^3 K^2 \eta^2 \sigma^2 + 4N^2 K^3 \eta^2 \sum_{s=1}^N \mathbb{E} \left[\left\| \nabla f_s(\mathbf{x}^r) \right\|^2 \right] + 4N^2 K^2 \eta^2 L^2 \mathcal{E} \quad (26)$$

Note that term \mathcal{E} is equivalent to $\sum_{i=1}^N \sum_{k=0}^{K-1} \mathbb{E} \left[\left\| \mathbf{x}_i^{(r,k)} - \mathbf{x}^r \right\|^2 \right]$, so we rearrange the equation and get:

$$(1 - 4N^2 K^2 \eta^2 L^2) \mathcal{E} \leq 2N^3 K^2 \eta^2 \sigma^2 + 4N^2 K^3 \eta^2 \sum_{s=1}^N \mathbb{E} \left[\left\| \nabla f_s(\mathbf{x}^r) \right\|^2 \right] \quad (27)$$

$$\stackrel{\text{Asm. 3}}{\leq} 2N^3 K^2 \eta^2 \sigma^2 + 4N^3 K^3 \eta^2 \left(B^2 \left\| \nabla f(\mathbf{x}^r) \right\|^2 + G^2 \right) \quad (28)$$

Using $4N^2 K^2 \eta^2 L^2 < 1$ and dividing both sides by $1 - 4N^2 K^2 \eta^2 L^2$ yields the claim of Lemma 4. \square

C.2 Proof of Theorem 1

Proof. Beginning with Assumption 1, we have

$$f(\mathbf{x}^{r+1}) - f(\mathbf{x}^r) \leq \langle \nabla f(\mathbf{x}^r), \mathbf{x}^{r+1} - \mathbf{x}^r \rangle + \frac{L}{2} \|\mathbf{x}^{r+1} - \mathbf{x}^r\|^2. \quad (29)$$

From Algorithm 1, we know $\mathbf{x}^{r+1} - \mathbf{x}^r = \mathbf{x}_N^{(r,K)} - \mathbf{x}^r = -\eta \sum_{i=1}^N \sum_{k=0}^{K-1} \mathbf{g}_i(\mathbf{x}_i^{(r,k)})$. Then for the expectation on \mathbf{x}^r , we have

$$\begin{aligned} & \mathbb{E}[f(\mathbf{x}^{r+1})] - f(\mathbf{x}^r) \\ & \leq \mathbb{E} \left[\left\langle \nabla f(\mathbf{x}^r), -\eta \sum_{i=1}^N \sum_{k=0}^{K-1} \mathbf{g}_i(\mathbf{x}_i^{(r,k)}) \right\rangle \right] + \frac{L}{2} \mathbb{E} \left[\left\| \eta \sum_{i=1}^N \sum_{k=0}^{K-1} \mathbf{g}_i(\mathbf{x}_i^{(r,k)}) \right\|^2 \right] \end{aligned} \quad (30)$$

$$= -N\eta \sum_{k=0}^{K-1} \mathbb{E} \left[\left\langle \nabla f(\mathbf{x}^r), \frac{1}{N} \sum_{i=1}^N \nabla f_i(\mathbf{x}_i^{(r,k)}) \right\rangle \right] + \frac{L}{2} \eta^2 \mathbb{E} \left[\left\| \sum_{i=1}^N \sum_{k=0}^{K-1} \mathbf{g}_i(\mathbf{x}_i^{(r,k)}) \right\|^2 \right], \quad (31)$$

where we use $\mathbb{E}[\mathbf{g}_i(\mathbf{x})] = \nabla f_i(\mathbf{x})$ in the equality (see Assumption 2). For the second term on the right hand side of Eq. (31), we have:

$$\begin{aligned} \mathbb{E} \left[\left\| \sum_{i=1}^N \sum_{k=0}^{K-1} \mathbf{g}_i(\mathbf{x}_i^{(r,k)}) \right\|^2 \right] & \stackrel{(6)}{\leq} 2\mathbb{E} \left[\left\| \sum_{i=1}^N \sum_{k=0}^{K-1} [\mathbf{g}_i(\mathbf{x}_i^{(r,k)}) - \nabla f_i(\mathbf{x}_i^{(r,k)})] \right\|^2 \right] \\ & \quad + 2\mathbb{E} \left[\left\| \sum_{i=1}^N \sum_{k=0}^{K-1} \nabla f_i(\mathbf{x}_i^{(r,k)}) \right\|^2 \right] \end{aligned} \quad (32)$$

$$\begin{aligned} & \stackrel{(8)}{\leq} 2\mathbb{E} \left[N \sum_{i=1}^N \left\| \sum_{k=0}^{K-1} [\mathbf{g}_i(\mathbf{x}_i^{(r,k)}) - \nabla f_i(\mathbf{x}_i^{(r,k)})] \right\|^2 \right] \\ & \quad + 2\mathbb{E} \left[\left\| \sum_{i=1}^N \sum_{k=0}^{K-1} \nabla f_i(\mathbf{x}_i^{(r,k)}) \right\|^2 \right] \end{aligned} \quad (33)$$

$$\begin{aligned} & \stackrel{\text{Lem. 3}}{\leq} 2\mathbb{E} \left[N \sum_{i=1}^N \sum_{k=0}^{K-1} \left\| \mathbf{g}_i(\mathbf{x}_i^{(r,k)}) - \nabla f_i(\mathbf{x}_i^{(r,k)}) \right\|^2 \right] \\ & \quad + 2\mathbb{E} \left[\left\| \sum_{i=1}^N \sum_{k=0}^{K-1} \nabla f_i(\mathbf{x}_i^{(r,k)}) \right\|^2 \right] \end{aligned} \quad (34)$$

$$\stackrel{\text{Asm. 2}}{\leq} 2N^2 K \sigma^2 + 2\mathbb{E} \left[\left\| \sum_{i=1}^N \sum_{k=0}^{K-1} \nabla f_i(\mathbf{x}_i^{(r,k)}) \right\|^2 \right]. \quad (35)$$

Note in Eq. (34) that we apply Jensen's Inequality to the first term on right hand side, since the data across clients are non-IID. Then plugging Eq. (35) into Eq. (31), we have

$$\begin{aligned} & \mathbb{E}[f(\mathbf{x}^{r+1})] - f(\mathbf{x}^r) \\ & \leq -N\eta \sum_{k=0}^{K-1} \mathbb{E} \left[\left\langle \nabla f(\mathbf{x}^r), \frac{1}{N} \sum_{i=1}^N \nabla f_i(\mathbf{x}_i^{(r,k)}) \right\rangle \right] + L\eta^2 \mathbb{E} \left[\left\| \sum_{i=1}^N \sum_{k=0}^{K-1} \nabla f_i(\mathbf{x}_i^{(r,k)}) \right\|^2 \right] \\ & \quad + N^2 K L \eta^2 \sigma^2 \end{aligned} \quad (36)$$

$$\begin{aligned} & = -\frac{N\eta}{2} \sum_{k=0}^{K-1} \left[\|\nabla f(\mathbf{x}^r)\|^2 + \mathbb{E} \left\| \frac{1}{N} \sum_{i=1}^N \nabla f_i(\mathbf{x}_i^{(r,k)}) \right\|^2 - \mathbb{E} \left\| \frac{1}{N} \sum_{i=1}^N \nabla f_i(\mathbf{x}_i^{(r,k)}) - \nabla f(\mathbf{x}^r) \right\|^2 \right] \\ & \quad + L\eta^2 \mathbb{E} \left[\left\| \sum_{i=1}^N \sum_{k=0}^{K-1} \nabla f_i(\mathbf{x}_i^{(r,k)}) \right\|^2 \right] + N^2 K L \eta^2 \sigma^2, \end{aligned} \quad (37)$$

where we use the fact that $2\langle a, b \rangle = \|a\|^2 + \|b\|^2 - \|a - b\|^2$ in the last equation. Note that

$$\begin{aligned} & -\frac{1}{2} N \eta \sum_{k=0}^{K-1} \mathbb{E} \left[\left\| \frac{1}{N} \sum_{i=1}^N \nabla f_i(\mathbf{x}_i^{(r,k)}) \right\|^2 \right] + L\eta^2 \mathbb{E} \left[\left\| \sum_{i=1}^N \sum_{k=0}^{K-1} \nabla f_i(\mathbf{x}_i^{(r,k)}) \right\|^2 \right] \\ & \stackrel{(8)}{\leq} -\frac{1}{2} \frac{1}{N} \eta \sum_{k=0}^{K-1} \mathbb{E} \left[\left\| \sum_{i=1}^N \nabla f_i(\mathbf{x}_i^{(r,k)}) \right\|^2 \right] + L\eta^2 K \sum_{k=0}^{K-1} \mathbb{E} \left[\left\| \sum_{i=1}^N \nabla f_i(\mathbf{x}_i^{(r,k)}) \right\|^2 \right] \\ & = -\frac{1}{2N} \eta (1 - 2NK L \eta) \sum_{k=0}^{K-1} \mathbb{E} \left[\left\| \sum_{i=1}^N \nabla f_i(\mathbf{x}_i^{(r,k)}) \right\|^2 \right] \end{aligned} \quad (38)$$

$$\begin{aligned} \text{and } \mathbb{E} \left[\left\| \frac{1}{N} \sum_{i=1}^N \nabla f_i(\mathbf{x}_i^{(r,k)}) - \nabla f(\mathbf{x}^r) \right\|^2 \right] & = \mathbb{E} \left[\left\| \frac{1}{N} \sum_{i=1}^N [\nabla f_i(\mathbf{x}_i^{(r,k)}) - \nabla f_i(\mathbf{x}^r)] \right\|^2 \right] \\ & \stackrel{(10)}{\leq} \frac{1}{N} \sum_{i=1}^N \mathbb{E} \left[\left\| \nabla f_i(\mathbf{x}_i^{(r,k)}) - \nabla f_i(\mathbf{x}^r) \right\|^2 \right] \\ & \stackrel{\text{Asm. 1}}{\leq} \frac{1}{N} \sum_{i=1}^N L^2 \mathbb{E} \left[\left\| \mathbf{x}_i^{(r,k)} - \mathbf{x}^r \right\|^2 \right], \end{aligned} \quad (39)$$

where the first equality of Eq. (39) results from the fact that $\nabla f(\mathbf{x}^r) = \frac{1}{N} \sum_{i=1}^N \nabla f_i(\mathbf{x}^r)$. By plugging Eq. (38) and Eq. (39) into Eq. (37) and using $2NK\eta L \leq 1$, we get

$$\mathbb{E}[f(\mathbf{x}^{r+1})] - f(\mathbf{x}^r) \leq -\frac{1}{2} NK \eta \|\nabla f(\mathbf{x}^r)\|^2 + \frac{1}{2} L^2 \eta \sum_{i=1}^N \sum_{k=0}^{K-1} \mathbb{E} \left[\left\| \mathbf{x}_i^{(r,k)} - \mathbf{x}^r \right\|^2 \right] + N^2 K L \eta^2 \sigma^2. \quad (40)$$

Then using Lemma 4, we have:

$$\begin{aligned} \frac{\mathbb{E}[f(\mathbf{x}^{r+1})] - f(\mathbf{x}^r)}{NK\eta} & \leq -\frac{1}{2} \left(1 - \frac{DB^2}{1-D} \right) \|\nabla f(\mathbf{x}^r)\|^2 + NL\eta\sigma^2 \\ & \quad + \frac{1}{1-D} (N^2 K L^2 \eta^2 \sigma^2 + 2N^2 K^2 L^2 \eta^2 G^2), \end{aligned} \quad (41)$$

where $D = 4N^2K^2L^2\eta^2$. Then using $D \leq \frac{1}{2B^2+1}$ and $B \geq 1$, we get

$$\begin{aligned} \frac{\mathbb{E}[f(\mathbf{x}^{r+1})] - f(\mathbf{x}^r)}{NK\eta} &\leq -\frac{1}{4} \|\nabla f(\mathbf{x}^r)\|^2 + NL\eta\sigma^2 + (1 + \frac{1}{2B^2}) (N^2KL^2\eta^2\sigma^2 + 2N^2K^2L^2\eta^2G^2) \\ &\leq -\frac{1}{4} \|\nabla f(\mathbf{x}^r)\|^2 + NL\eta\sigma^2 + \frac{3}{2}N^2KL^2\eta^2\sigma^2 + 3N^2K^2L^2\eta^2G^2 \end{aligned} \quad (42)$$

Taking unconditional expectation, rearranging the terms and then averaging the above equation over $r = \{0, \dots, R-1\}$, we have

$$\frac{1}{R} \sum_{r=0}^{R-1} \mathbb{E} [\|\nabla f(\mathbf{x}^r)\|^2] \leq \frac{4[f(\mathbf{x}^0) - f(\mathbf{x}^*)]}{NK\eta R} + 12N^2K^2\eta^2L^2G^2 + 6N^2K\eta^2L^2\sigma^2 + 4N\eta L\sigma^2$$

Using the fact that $\mathbb{E} [\|\nabla f(\bar{\mathbf{x}}^R)\|^2] \leq \frac{1}{R} \sum_{r=0}^{R-1} \mathbb{E} [\|\nabla f(\mathbf{x}^r)\|^2]$ where $\bar{\mathbf{x}}^R = \frac{1}{R} \sum_{r=0}^{R-1} \mathbf{x}^r$, we get Eq. (4). Finally, we summarize the constraints:

$$D = 4N^2K^2L^2\eta^2 \leq \frac{1}{2B^2+1} \quad (43)$$

$$2NK\eta L \leq 1 \quad (44)$$

where the last inequality is from Lemma 4. The overall constraint is given as:

$$\eta \leq \frac{1}{2NK L \sqrt{2B^2+1}} \quad (45)$$

Now we complete the proof of Theorem 1. \square

C.3 Proof of Theorem 2

Theorem 2. Let Assumptions 1, 2 and 3 hold. Suppose that the local learning rate satisfies $\eta_l \leq \frac{1}{2KL} \min \left\{ \frac{1}{\sqrt{2B^2+1}}, \frac{1}{\eta_g} \right\}$. For Algorithm 1, it holds that

$$\mathbb{E} [\|\nabla f(\bar{\mathbf{x}}^R)\|^2] \leq \underbrace{\frac{4[f(\mathbf{x}^0) - f(\mathbf{x}^*)]}{K\eta_g\eta_l R}}_{T_1: \text{initialization error}} + \underbrace{12K(K-1)\eta_l^2L^2G^2 + 6(K-1)\eta_l^2L^2\sigma^2}_{T_2: \text{client drift error}} + \underbrace{\frac{4\eta_g\eta_l L\sigma^2}{N}}_{T_3: \text{global variance}}, \quad (46)$$

where $\bar{\mathbf{x}}^R = \frac{1}{R} \sum_{r=0}^{R-1} \mathbf{x}^r$ is the averaged global model over the R rounds.

Proof. This is almost the same as Theorem 1 of Wang et al. (2020), we reproduce here for convenience of comparison between FL and SL. The proof is similar to that of Theorem 1. \square

C.4 Proof of Theorem 3

Here we use Assumption 4 to replace Assumption 3, one stronger assumption (than Assumption 3) used in Lian et al. (2017).

Assumption 4. There exist constants $G \geq 0$ such that

$$\mathbb{E}_{i \sim \mathcal{U}([N])} [\|\nabla f_i(\mathbf{x}) - \nabla f(\mathbf{x})\|] \leq G^2, \quad (47)$$

where i is uniformly sampled from $\{1, \dots, N\}$. In the IID case, $G = 0$.

Theorem 3 (Progress of one client in one round). *Let Assumptions 1, 2 and 3 hold. Suppose that the local learning rate satisfies $\eta \leq \frac{1}{2\sqrt{5}KL}$. For Algorithm 1, it holds that*

$$\begin{aligned} \frac{1}{NR} \sum_{r=0}^{R-1} \sum_{i=1}^N \mathbb{E} \left[\left\| \nabla f(\mathbf{x}_i^{(r,0)}) \right\|^2 \right] &\leq \frac{4[f(\mathbf{x}^0) - f(\mathbf{x}^*)]}{NK\eta R} + 40K^2L^2\eta^2G^2 \\ &\quad + 10KL^2\eta^2\sigma^2 + 4L\eta\sigma^2 + 4G^2. \end{aligned} \quad (48)$$

Proof. Different from Theorem 1, we bound the progress of one client in one round. Beginning with Assumption 1, we have:

$$\mathbb{E} \left[f(\mathbf{x}_{i+1}^{(r,0)}) - f(\mathbf{x}_i^{(r,0)}) \right] \leq \mathbb{E} \left[\left\langle \nabla f(\mathbf{x}_i^{(r,0)}), \mathbf{x}_{i+1}^{(r,0)} - \mathbf{x}_i^{(r,0)} \right\rangle \right] + \frac{L}{2} \mathbb{E} \left[\left\| \mathbf{x}_{i+1}^{(r,0)} - \mathbf{x}_i^{(r,0)} \right\|^2 \right] \quad (49)$$

From Algorithm 1, we know the local update of client i in round r can be written as:

$$\mathbf{x}_{i+1}^{(r,0)} - \mathbf{x}_i^{(r,0)} = -\eta \sum_{k=0}^{K-1} \mathbf{g}_i(\mathbf{x}_i^{(r,k)}). \quad (50)$$

For the expectation on $\mathbf{x}_i^{(r,0)}$, we get

$$\begin{aligned} &\mathbb{E} \left[f(\mathbf{x}_{i+1}^{(r,0)}) - f(\mathbf{x}_i^{(r,0)}) \right] \\ &\leq \mathbb{E} \left[\left\langle \nabla f(\mathbf{x}_i^{(r,0)}), -\eta \sum_{k=0}^{K-1} \mathbf{g}_i(\mathbf{x}_i^{(r,k)}) \right\rangle \right] + \frac{L}{2} \mathbb{E} \left[\left\| \eta \sum_{k=0}^{K-1} \mathbf{g}_i(\mathbf{x}_i^{(r,k)}) \right\|^2 \right] \end{aligned} \quad (51)$$

$$= -\eta \sum_{k=0}^{K-1} \mathbb{E} \left[\left\langle \nabla f(\mathbf{x}_i^{(r,0)}), \nabla f_i(\mathbf{x}_i^{(r,k)}) \right\rangle \right] + \frac{L}{2} \eta^2 \mathbb{E} \left[\left\| \sum_{k=0}^{K-1} \mathbf{g}_i(\mathbf{x}_i^{(r,k)}) \right\|^2 \right], \quad (52)$$

where we use $\mathbb{E}[\mathbf{g}_i(\mathbf{x})] = \nabla f_i(\mathbf{x})$ in the equality (see Assumption 2). For the second term on the right hand side of Eq. (52), we have:

$$\begin{aligned} \mathbb{E} \left[\left\| \sum_{k=0}^{K-1} \mathbf{g}_i(\mathbf{x}_i^{(r,k)}) \right\|^2 \right] &\stackrel{(6)}{\leq} 2\mathbb{E} \left[\left\| \sum_{k=0}^{K-1} \left[\mathbf{g}_i(\mathbf{x}_i^{(r,k)}) - \nabla f_i(\mathbf{x}_i^{(r,k)}) \right] \right\|^2 \right] \\ &\quad + 2\mathbb{E} \left[\left\| \sum_{k=0}^{K-1} \nabla f_i(\mathbf{x}_i^{(r,k)}) \right\|^2 \right] \end{aligned} \quad (53)$$

$$\begin{aligned} &\stackrel{\text{Lem. 3}}{\leq} 2\mathbb{E} \left[\sum_{k=0}^{K-1} \left\| \mathbf{g}_i(\mathbf{x}_i^{(r,k)}) - \nabla f_i(\mathbf{x}_i^{(r,k)}) \right\|^2 \right] \\ &\quad + 2\mathbb{E} \left[\left\| \sum_{k=0}^{K-1} \nabla f_i(\mathbf{x}_i^{(r,k)}) \right\|^2 \right] \end{aligned} \quad (54)$$

$$\stackrel{\text{Asm. 2}}{\leq} 2K\sigma^2 + 2\mathbb{E} \left[\left\| \sum_{k=0}^{K-1} \nabla f_i(\mathbf{x}_i^{(r,k)}) \right\|^2 \right]. \quad (55)$$

Then plugging Eq. (55) into Eq. (52), we have:

$$\begin{aligned} & \mathbb{E} \left[f(\mathbf{x}_{i+1}^{(r,0)}) - f(\mathbf{x}_i^{(r,0)}) \right] \\ & \leq -\eta \sum_{k=0}^{K-1} \mathbb{E} \left[\left\langle \nabla f(\mathbf{x}_i^{(r,0)}), \nabla f_i(\mathbf{x}_i^{(r,k)}) \right\rangle \right] + L\eta^2 \mathbb{E} \left[\left\| \sum_{k=0}^{K-1} \nabla f_i(\mathbf{x}_i^{(r,k)}) \right\|^2 \right] + KL\eta^2 \sigma^2 \end{aligned} \quad (56)$$

$$\begin{aligned} & = -\frac{\eta}{2} \sum_{k=0}^{K-1} \left[\left\| \nabla f(\mathbf{x}_i^{(r,0)}) \right\|^2 + \mathbb{E} \left\| \nabla f_i(\mathbf{x}_i^{(r,k)}) \right\|^2 - \mathbb{E} \left\| \nabla f_i(\mathbf{x}_i^{(r,k)}) - \nabla f(\mathbf{x}_i^{(r,0)}) \right\|^2 \right] \\ & \quad + L\eta^2 \mathbb{E} \left[\left\| \sum_{k=0}^{K-1} \nabla f_i(\mathbf{x}_i^{(r,k)}) \right\|^2 \right] + KL\eta^2 \sigma^2, \end{aligned} \quad (57)$$

where we use the fact that $2 \langle a, b \rangle = \|a\|^2 + \|b\|^2 - \|a - b\|^2$ in the last equation. Note that

$$\begin{aligned} & -\frac{1}{2}\eta \sum_{k=0}^{K-1} \mathbb{E} \left[\left\| \nabla f_i(\mathbf{x}_i^{(r,k)}) \right\|^2 \right] + L\eta^2 \mathbb{E} \left[\left\| \sum_{k=0}^{K-1} \nabla f_i(\mathbf{x}_i^{(r,k)}) \right\|^2 \right] \\ & \stackrel{(8)}{\leq} -\frac{1}{2}\eta \sum_{k=0}^{K-1} \mathbb{E} \left[\left\| \nabla f_i(\mathbf{x}_i^{(r,k)}) \right\|^2 \right] + L\eta^2 K \sum_{k=0}^{K-1} \mathbb{E} \left[\left\| \nabla f_i(\mathbf{x}_i^{(r,k)}) \right\|^2 \right] \\ & = -\frac{1}{2}\eta(1 - 2KL\eta) \sum_{k=0}^{K-1} \mathbb{E} \left[\left\| \nabla f_i(\mathbf{x}_i^{(r,k)}) \right\|^2 \right] \end{aligned} \quad (58)$$

$$\begin{aligned} \text{and } \mathbb{E} \left[\left\| \nabla f_i(\mathbf{x}_i^{(r,k)}) - \nabla f(\mathbf{x}_i^{(r,0)}) \right\|^2 \right] & = 2\mathbb{E} \left[\left\| \nabla f_i(\mathbf{x}_i^{(r,k)}) - \nabla f_i(\mathbf{x}_i^{(r,0)}) \right\|^2 \right] \\ & \quad + 2\mathbb{E} \left[\left\| \nabla f_i(\mathbf{x}_i^{(r,0)}) - \nabla f(\mathbf{x}_i^{(r,0)}) \right\|^2 \right] \end{aligned} \quad (59)$$

$$\stackrel{\text{Asm. 1}}{\leq} 2L^2 \mathbb{E} \left[\left\| \mathbf{x}_i^{(r,k)} - \mathbf{x}_i^{(r,0)} \right\|^2 \right] + 2G^2. \quad (60)$$

By plugging Eq. (58) and Eq. (60) into Eq. (57) and using $2K\eta L \leq 1$, we get

$$\begin{aligned} \mathbb{E} \left[f(\mathbf{x}_{i+1}^{(r,0)}) - f(\mathbf{x}_i^{(r,0)}) \right] & \leq -\frac{1}{2}K\eta \left\| \nabla f(\mathbf{x}_i^{(r,0)}) \right\|^2 + L^2\eta \sum_{k=0}^{K-1} \mathbb{E} \left[\left\| \mathbf{x}_i^{(r,k)} - \mathbf{x}_i^{(r,0)} \right\|^2 \right] \\ & \quad + K\eta G^2 + KL\eta^2 \sigma^2. \end{aligned} \quad (61)$$

Then using the bounded client-drift in Wang et al. (2020), i.e.,

$$\sum_{k=0}^{K-1} \mathbb{E} \left[\left\| \mathbf{x}_i^{(r,k)} - \mathbf{x}_i^{(r,0)} \right\|^2 \right] \leq \frac{4K^3\eta^2 \left\| \nabla f_i(\mathbf{x}_i^{(r,0)}) \right\|^2 + 2K^2\eta^2 \sigma^2}{1 - 4K^2L^2\eta^2}, \quad (62)$$

we can get

$$\begin{aligned} \frac{\mathbb{E} \left[f(\mathbf{x}_{i+1}^{(r,0)}) - f(\mathbf{x}_i^{(r,0)}) \right]}{K\eta} & \leq -\frac{1}{2} \left(1 - \frac{2D}{1-D} \right) \left\| \nabla f(\mathbf{x}_i^{(r,0)}) \right\|^2 + L\eta\sigma^2 + G^2 \\ & \quad + \frac{2D}{1-D}G^2 + \frac{2KL^2\eta^2\sigma^2}{1-D}, \end{aligned} \quad (63)$$

where $D = 4K^2L^2\eta^2$. Then using $D \leq \frac{1}{5}$ ($\frac{1}{1-D} \leq \frac{5}{4}$) and $B \geq 1$, we get

$$\begin{aligned} \frac{\mathbb{E} \left[f(\mathbf{x}_{i+1}^{(r,0)}) - f(\mathbf{x}_i^{(r,0)}) \right]}{K\eta} &\leq -\frac{1}{4} \left\| \nabla f(\mathbf{x}_i^{(r,0)}) \right\|^2 + L\eta\sigma^2 + G^2 \\ &\quad + \frac{5}{2}KL^2\eta^2\sigma^2 + 10K^2L^2\eta^2G^2 \end{aligned} \quad (64)$$

Taking unconditional expectation, rearranging the terms and then averaging the above equation over $i = \{1, \dots, N\}, r = \{0, \dots, R-1\}$, we have

$$\begin{aligned} \frac{1}{NR} \sum_{r=0}^{R-1} \sum_{i=1}^N \mathbb{E} \left[\left\| \nabla f(\mathbf{x}_i^{(r,0)}) \right\|^2 \right] &\leq \frac{4[f(\mathbf{x}^0) - f(\mathbf{x}^*)]}{NK\eta R} + 40K^2L^2\eta^2G^2 \\ &\quad + 10KL^2\eta^2\sigma^2 + 4L\eta\sigma^2 + 4G^2 \end{aligned} \quad (65)$$

Finally, we summarize the constraints:

$$D = 4K^2L^2\eta^2 \leq \frac{1}{5} \quad (66)$$

$$2K\eta L \leq 1. \quad (67)$$

The overall constraint is given as:

$$\eta \leq \frac{1}{2\sqrt{5}KL} \quad (68)$$

Now we complete the proof of Theorem 1. □

D More experimental details

Platform. We train LeNet-5 on MNIST and Fashion-MNIST with Nvidia GeForce RTX 3070 Ti, VGG-11 on CIFAR-10 with Nvidia 3090 Ti. The algorithms are implemented by PyTorch. We use the random seed “1234” by default. We use vanilla SGD algorithm with momentum = 0.9 and weight decay = 1e-4 as He et al. (2020). The detailed information of the models and other information can be found in our code.

D.1 More results of SL

This section is complimentary to Section 5.2 to study the factors that affects the performance of SL. We report the details of the experiments, such as η_l , η_g , b .

Effect of data heterogeneity.

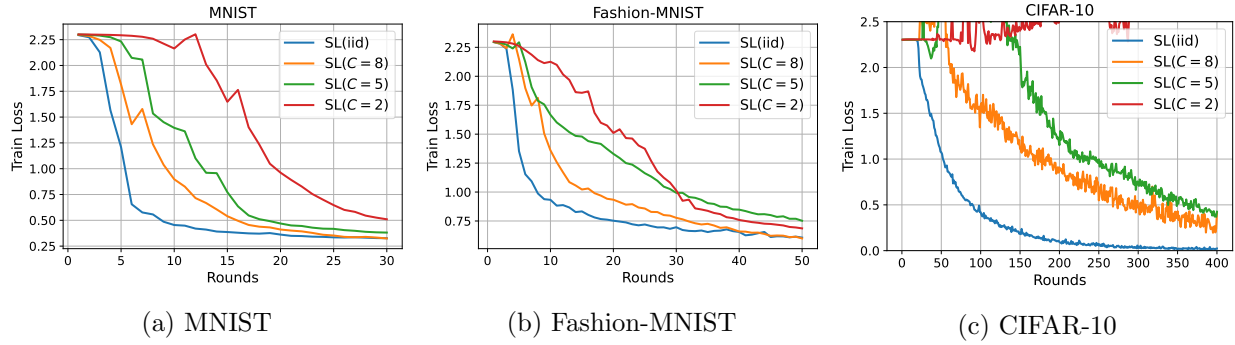


Figure 5: Effect of data heterogeneity. (a) MNIST, $N = 10$, $b = 1000$, $\eta_l = 0.01$, $\eta_g = 1.0$; (b) Fashion-MNIST, $N = 10$, $b = 1000$, $\eta_l = 0.01$, $\eta_g = 1.0$; (c) CIFAR-10, $N = 10$, $b = 100$, $\eta_l = 0.001$, $\eta_g = 1.0$.

Effect of K .

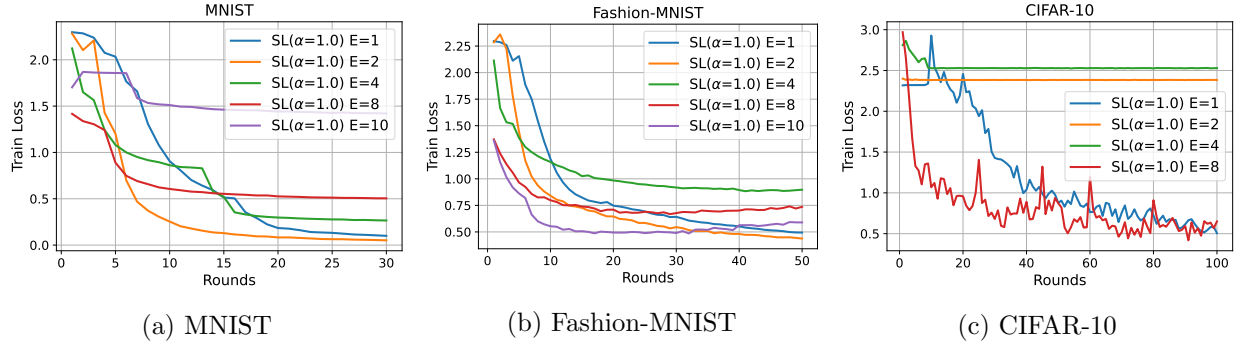


Figure 6: Effect of K . $\text{Dir}_{10}(1.0)$ is used. (a) MNIST, $N = 10$, $b = 1000$, $\eta_l = 0.01$, $\eta_g = 1.0$; (b) Fashion-MNIST, $N = 10$, $b = 1000$, $\eta_l = 0.01$, $\eta_g = 1.0$; (c) CIFAR-10, $N = 10$, $b = 100$, $\eta_l = 0.005$, $\eta_g = 1.0$.

D.2 More comparisons between FL and SL in cross-device setting

The learning rates of FL and SL are selected from $\{0.0005, 0.001, 0.005, 0.01, 0.05, 0.1\}$. We report the overall results of comparisons between FL and SL on MNIST, Fashion-MNIST and CIFAR-10 datasets with different learning rates in Table 6, Table 7 and Table 8 respectively. Table 2 in the

main body are based on these three tables here. “L-M”, “L-M” and “V-10” denote LeNet-5 on MNIST, LeNet-5 on Fashion-MNIST and VGG-11 on CIFAR-10 respectively. We highlight the “best” test accuracy among all chosen learning rates with blue for FL and red for SL. We underline the test accuracy of the “threshold” learning rate with blue for FL and red for SL.

Table 6: The detailed results of FL and SL with different learning rates on MNIST dataset. We average the test accuracy over the last 100 rounds from 1000 total rounds when $E = 1$; average the test accuracy over the last 10 rounds from 100 total rounds when $E = 10$.

Tag	N	Dist.	E	b	0.0005		0.001		0.005		0.01		0.05		0.1	
					FL	SL	FL	SL	FL	SL	FL	SL	FL	SL	FL	SL
L-M	1000	IID	1	10	67.8	97.8	92.0	98.4	98.3	98.9	98.7	89.2	<u>99.0</u>	<u>11.3</u>	99.0	11.3
L-M	1000	$\alpha = 10.0$	1	10	78.1	98.3	93.2	98.7	98.5	99.0	98.7	98.9	<u>99.0</u>	<u>11.3</u>	98.7	11.3
L-M	1000	$\alpha = 5.0$	1	10	80.2	97.9	93.4	98.7	98.5	98.9	98.8	98.9	<u>99.1</u>	<u>11.3</u>	98.8	11.3
L-M	1000	$\alpha = 0.5$	1	10	81.3	97.9	93.6	98.6	98.4	98.8	98.8	98.7	<u>98.9</u>	<u>11.3</u>	98.3	11.3
L-M	1000	$\alpha = 0.2$	1	10	85.9	98.3	94.0	98.6	98.3	98.8	98.7	98.7	<u>98.7</u>	<u>11.3</u>	<u>11.3</u>	11.3
L-M	1000	$C = 5$	1	10	65.3	98.3	91.6	98.6	98.3	98.9	98.7	98.9	<u>99.0</u>	<u>11.3</u>	98.9	11.3
L-M	1000	$C = 2$	1	10	56.4	98.2	89.2	98.6	97.9	99.0	98.5	99.0	<u>98.8</u>	<u>11.3</u>	98.8	11.3
L-M	1000	IID	10	10	93.4	97.3	95.6	87.9	97.6	97.6	<u>97.9</u>	96.2	95.5	<u>11.3</u>	<u>11.3</u>	11.3
L-M	1000	$\alpha = 10.0$	10	10	93.8	97.5	96.2	97.5	<u>97.4</u>	97.4	97.4	39.4	<u>11.3</u>	<u>11.3</u>	11.3	11.3
L-M	1000	$\alpha = 5.0$	10	10	93.9	88.3	96.2	97.8	97.8	69.3	<u>98.0</u>	<u>11.3</u>	<u>11.3</u>	11.3	11.3	11.3
L-M	1000	$\alpha = 0.5$	10	10	92.6	87.9	94.9	97.9	97.3	<u>11.3</u>	<u>97.9</u>	11.3	<u>11.3</u>	11.3	11.3	11.3
L-M	1000	$\alpha = 0.2$	10	10	82.9	96.7	93.4	96.8	96.5	95.6	<u>96.8</u>	<u>11.4</u>	<u>11.3</u>	11.3	11.3	11.3
L-M	1000	$C = 5$	10	10	91.9	88.3	95.0	98.0	97.7	77.7	<u>98.0</u>	<u>11.3</u>	<u>9.8</u>	11.3	11.3	11.3
L-M	1000	$C = 2$	10	10	70.8	96.9	88.4	97.1	<u>96.8</u>	<u>11.3</u>	87.6	11.3	<u>11.3</u>	11.3	11.3	11.3

Table 7: The detailed results of FL and SL with different learning rates on Fashion-MNIST dataset. We average the test accuracy over the last 100 rounds from 1000 total rounds when $E = 1$; average the test accuracy over the last 10 rounds from 100 total rounds when $E = 10$.

Tag	N	Dist.	E	b	0.0005		0.001		0.005		0.01		0.05		0.1	
					FL	SL	FL	SL	FL	SL	FL	SL	FL	SL	FL	SL
L-F	1000	IID	1	10	54.4	75.0	68.8	85.9	83.7	88.4	86.1	88.2	<u>88.1</u>	82.4	87.8	<u>10.0</u>
L-F	1000	$\alpha = 10.0$	1	10	57.4	84.0	71.0	86.5	84.4	88.8	86.4	88.6	<u>88.1</u>	80.2	87.5	<u>10.2</u>
L-F	1000	$\alpha = 5.0$	1	10	57.4	84.6	74.0	86.3	84.2	88.6	86.3	88.4	<u>88.2</u>	79.9	87.6	<u>10.0</u>
L-F	1000	$\alpha = 0.5$	1	10	59.3	83.4	72.9	85.4	83.0	87.6	85.2	87.3	<u>86.7</u>	15.6	85.2	<u>10.0</u>
L-F	1000	$\alpha = 0.2$	1	10	60.8	81.6	71.3	84.3	80.8	85.9	<u>83.5</u>	84.9	83.4	<u>10.0</u>	<u>10.0</u>	10.0
L-F	1000	$C = 5$	1	10	53.8	82.4	67.0	85.6	81.7	88.0	84.6	88.1	<u>87.5</u>	<u>10.0</u>	86.8	10.0
L-F	1000	$C = 2$	1	10	50.9	80.4	62.6	83.9	77.5	87.3	76.5	86.6	81.1	<u>10.0</u>	<u>83.0</u>	10.0
L-F	1000	IID	10	10	75.6	82.7	78.8	84.0	84.0	82.5	<u>85.0</u>	80.0	46.4	<u>11.0</u>	<u>10.0</u>	10.0
L-F	1000	$\alpha = 10.0$	10	10	76.0	83.6	79.4	84.1	84.0	81.7	<u>84.8</u>	63.7	<u>10.0</u>	<u>10.0</u>	10.0	10.0
L-F	1000	$\alpha = 5.0$	10	10	76.0	83.2	79.5	76.6	83.9	80.8	<u>84.5</u>	77.0	<u>10.0</u>	<u>10.0</u>	10.0	10.0
L-F	1000	$\alpha = 0.5$	10	10	72.7	78.0	75.8	79.2	82.8	76.8	<u>83.8</u>	<u>10.0</u>	<u>10.0</u>	10.0	10.0	10.0
L-F	1000	$\alpha = 0.2$	10	10	65.1	79.0	68.4	78.6	79.3	70.9	<u>80.4</u>	<u>10.0</u>	<u>10.0</u>	10.0	10.0	10.0
L-F	1000	$C = 5$	10	10	68.6	78.9	72.7	80.1	80.6	77.5	<u>82.7</u>	25.8	78.0	<u>10.0</u>	<u>10.0</u>	10.0
L-F	1000	$C = 2$	10	10	52.8	72.0	59.5	72.3	73.3	<u>10.0</u>	<u>75.9</u>	10.0	34.5	10.0	<u>10.0</u>	10.0

Table 8: The detailed results of FL and SL with different learning rates on CIFAR-10 dataset. We average the test accuracy over the last 400 rounds from 4000 total rounds when $E = 1$; average the test accuracy over the last 40 rounds from 400 total rounds when $E = 10$. We don not execute the experiments whose learning rates are larger than the “threshold” learning rate (“-” in the table).

Tag	N	Dist.	E	b	0.0005		0.001		0.005		0.01		0.05		0.1	
					FL	SL	FL	SL	FL	SL	FL	SL	FL	SL	FL	SL
V-10	500	IID	1	10	-	-	43.1	86.2	84.0	87.0	85.5	85.1	86.4	10.0	10.0	10.0
V-10	500	$\alpha = 10.0$	1	10	-	-	47.4	86.4	84.2	86.9	85.7	84.2	86.3	10.0	10.0	-
V-10	500	$\alpha = 5.0$	1	10	-	-	47.2	86.5	84.2	87.0	85.6	84.5	86.1	10.0	10.0	-
V-10	500	$\alpha = 0.5$	1	10	-	-	44.5	85.4	82.1	85.5	84.1	10.0	10.0	-	-	-
V-10	500	$\alpha = 0.2$	1	10	22.9	81.2	39.4	83.5	78.1	83.0	80.5	10.0	10.0	-	-	-
V-10	500	$C = 5$	1	10	14.4	83.7	37.6	85.9	82.3	86.5	84.7	83.4	85.5	-	10.0	10.0
V-10	500	$C = 2$	1	10	14.0	81.9	23.9	84.7	73.7	84.7	79.2	12.9	80.0	10.0	10.0	-
V-10	500	IID	10	10	51.5	83.2	68.3	83.7	77.3	78.3	77.7	10.0	10.0	10.0	10.0	10.0
V-10	500	$\alpha = 10.0$	10	10	53.3	82.8	69.1	83.0	76.3	10.0	77.9	10.0	10.0	-	10.0	-
V-10	500	$\alpha = 5.0$	10	10	54.2	82.1	68.1	82.7	77.6	10.0	76.9	10.0	10.0	-	-	-
V-10	500	$\alpha = 0.5$	10	10	40.6	75.1	58.4	76.9	71.0	10.0	71.8	10.0	10.0	10.0	10.0	10.0
V-10	500	$\alpha = 0.2$	10	10	27.1	65.0	41.0	10.0	66.2	10.0	66.9	10.0	10.0	10.0	10.0	10.0
V-10	500	$C = 5$	10	10	36.3	77.6	59.6	78.9	73.9	10.0	74.2	-	10.0	-	10.0	-
V-10	500	$C = 2$	10	10	20.3	58.7	27.8	10.0	51.8	10.0	61.6	-	10.0	-	10.0	-